

**SENSORLESS VECTOR CONTROL OF PERMANENT  
MAGNET SYNCHRONOUS MACHINE  
DISSERTATION  
SUBMITTED IN PARTIAL FULFILLMENT OF THE  
REQUIREMENTS  
FOR THE AWARD OF THE DEGREE  
OF  
MASTER OF TECHNOLOGY  
IN  
POWER SYSTEM ENGINEERING**

**Submitted by**

**Pratyush Kumar Dwivedi**

**(2K18/PSY/06)**

**Under the guidance of**

**PROF. MUKHTIAR SINGH**



**Electrical Engineering Department  
DELHI TECHNOLOGICAL UNIVERSITY  
Shahbad Daultapur, Delhi-110042  
December, 2020**

# DELHI TECHNOLOGICAL UNIVERSITY

(Formerly Delhi College of Engineering)

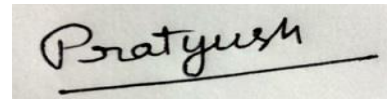
Bawana Road, Delhi-110042

## CANDIDATE'S DECLARATION

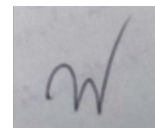
I, PRATYUSH KUMAR DWIVEDI, Roll No. 2K18/PSY/06 student of M.Tech (Power System), hereby declare that the major project report titled "Sensorless Vector Control Of Permanent Magnet Synchronus Machine" which is submitted by me to the Department of Electrical Engineering, Delhi Technological University, Delhi in partial fulfillment of the requirement for the award of the degree of Master of Technology has not been submitted elsewhere for the award of any Degree.

Place: Delhi

Date: 26/08/2020



PRATYUSH KUMAR DWIVEDI



**Prof. Mukhtiar Singh**

**(SUPERVISOR)**

Professor

Department of Electrical Engineering

Delhi Technological University

## **ACKNOWLEDGEMENT**

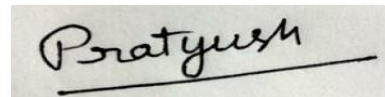
I am highly grateful to the Department of Electrical Engineering, Delhi Technological University (DTU) for providing this opportunity to carry out this project work.

The constant guidance and encouragement received from my supervisor Prof. Mukhtiar Singh of Department of Electrical Engineering, DTU, has been of great help in carrying my present work and is acknowledged with reverential thanks.

I would like to thank Mr. Akash Seth (PhD scholar), Mr Kailash Rana (Phd Scholar) for their guidance and continuous support in completion of this project work.

I would like to express my gratitude towards all the people who have contributed their precious time and effort to help me without whom it would not have been possible for me to understand and complete the project.

Finally, I would like to express gratitude to all faculty members of Electrical Engineering Department, DTU for their intellectual support in my M.tech study at DTU.

A rectangular box containing a handwritten signature in black ink. The signature is written in a cursive style and reads "Pratyush". A horizontal line is drawn underneath the signature.

Date :26/08/2020

PRATYUSH KUMAR DWIVEDI

## **ABSTRACT**

The main of this project is to implement different sensorless techniques for sensorless vector control of PMSM. A modified SMO based sensorless control is presented, which improves the performance of motor. Further, the performance is improved with MARS based sensorless technique.

SMO are known for their robust nature against the parameter variation and disturbance due to which they are preferred choice in sensorless control. Conventionally SMO is used with signum function but chattering is a major problem in sliding mode . In this project, SMO is used with saturation function to mitigate the effect of chattering. But the presence of lpf deteriorates the dynamic performance of SMO as it introduces the time delay in the system. Hence, a modified SMO is designed with back emf observer. Further, the performance is improved with a MARS based sensorless technique . The sliding mode controller is used as adaptive law to improve the performance.

# **TABLE OF CONTENTS**

<b>CONTENT</b>		<b>PAGE NUMBER</b>
	Candidate declaration	<b>i</b>
	Certificate	<b>ii</b>
	Acknowledgment	<b>iii</b>
	Abstract	<b>iv</b>
CHAPTER 1	1.1 Introduction	
	1.2 Background	
	1.3 Problem Definition	
	1.4 Scope	
	1.5 Methodology	
	1.6 Content	
CHAPTER 2	2.1 Literature Survey	
	2.2. Sliding Mode Observer	

2.3. Model Adaptive Reference System

2.4. Extended Kalman Filter

2.5. Flux Observer Method

2.6. Discussion

## CHAPTER 3

3.1. Permanent Magnet Synchronous Machine

3.1.1. abc frame

3.1.2. alpha- beta frame

3.1.3. dq frame

3.2 Field Oriented Control

3.3 Space Vector Modulation

## CHAPTER 4

Sensored Control

4.1. Sensored Control

4.2. PI Control Design

4.3 Simulation

## CHAPTER 5

Sensorless Control

5.1. Sensorless Control

## 5.2. Sliding mode observer(SMO)

### 5.2.1. Mathematical Modelling

### 5.2.2. Stability Analysis

### 5.2.3. Phase compensation module

### 5.2.4. Rotor velocity estimation

### 5.2.5. Simulation

## 5.3. Improved Modified SMO

### 5.3.1 Sigmoid as a switching function

### 5.3.2. Mathematical Modelling

### 5.3.3. Stability Analysis

### 5.3.4. Estimation of Rotor position and speed

### 5.3.5. Simulation

## CHAPTER 6

### 6.1. Model Reference Adaptive System

### 6.2. Mathematical Modelling

6.3. Stability Analysis

6.4. Simulation

6.5. Discussion

CHAPTER 7

7.1 CONCLUSION

7.2. FUTURE WORK

References



## List of Figures

<u>Figure no</u>	<u>Description</u>
3.1	Equivalent Circuit Of A Motor In dq0 Phase
3.2	Field Oriented Control Of Pmsm
3.3	Space Vector Representation Of Inverter
4.1	Iq Current Loop With An External Disturbance
4.2	Simplified Iq Loop
4.3	Rotor Velocity Response When Speed Reference Is Changed From 200 Rpm To 750 Rpm
4.4	Electromagnetic Torque When Speed Reference Is Changed From 200 Rpm To 750 Rpm
4.5	Id Current When Speed Reference Is Changed From 200 Rpm To 750 Rpm
4.6	Iq Current When Speed Reference Is Changed From 200 Rpm To 750 Rpm For The Rated Load Torque Of 20 Nm
4.7	Electromagnetic Torque When The Torque Load Is Changed From 20 Nm To 10 Nm With Rated Speed Of 750 Rpm
4.8	Rotor Velocity When The Torque Load Is Changed From 20 Nm To 10 Nm With Rated Speed Of 750 Rpm
4.9	Iq Current When The Torque Load Is Changed From 20 Nm To 10 Nm With Rated Speed Of 750 Rpm

- 4.10 Id Current When The Torque Load Is Changed From 20 Nm To 10 Nm With Rated Speed Of 750 Rpm
- 5.1 Sensorless Control
- 5.2 Saturation Function
- 5.3 Simulated Sliding mode observer
- 5.4 Rotor velocity
- 5.5 Electromagnetic Torque
- 5.6 Id Current When The Reference Is Set To Zero
- 5.7 Iq Current
- 5.8 Rotor Velocity
- 5.9 Electromagnetic Torque When The Speed Reference Is Changed From 400 Rpm To 750 Rpm At 1 Second
- 5.10 Electrical Rotor Angle When Speed Reference Is Changed From 400 Rpm To 750 Rpm At 1 Second
- 5.11 Electrical Rotor Angle Error B/W The Actual Rotor Angle And Smo Rotor Angle When Speed Reference Is Changed From 400 Rpm To 750 Rpm At 1 Second.
- 5.12 Rotor angle of the pmsm motor
- 5.13 Rotor Angle Error

- 5.14  $i_{\alpha}, i_{\beta}$  Of The Pmsm At 750 Rpm I.E. Current In The Stator At 50 Hz
- 5.15  $\hat{i}_{\alpha}, \hat{i}_{\beta}$  Of The Pmsm At 750 Rpm I.E. Current In The Stator At 50 Hz
- 5.16  $\widehat{e}_{\alpha}, \widehat{e}_{\beta}$  Of The Pmsm At 750 Rpm I.E. Current In The Stator At 50 Hz
- 5.17  $i_{\alpha}, i_{\beta}$  Of The Pmsm At 400 Rpm I.E. Current In The Stator At 26.66 Hz
- 5.18  $\hat{i}_{\alpha}, \hat{i}_{\beta}$  Of The Pmsm At 400 Rpm I.E. Current In The Stator At 26.66 Hz
- 5.19  $\widehat{e}_{\alpha}, \widehat{e}_{\beta}$  Of The Pmsm At 400 Rpm I.E. Current In The Stator At 26.66 Hz
- 5.20 Sigmoid as a switching function
- 5.21 Simulated Sliding Mode Observer
- 5.22 Rotor Velocity
- 5.23 Id Current
- 5.24 Iq Current
- 5.25 Electromagnetic Torque
- 5.26 Rotor Velocity
- 5.27 Electromagnetic Torque (Te)
- 5.28 Rotor Angle

- 5.29 Estimated Rotor Angle Error
- 5.30 Electromagnetic Torque
- 5.31 Rotor Velocity
- 5.32 Rotor Angle
- 5.33 Estimated Rotor Angle Error
- 5.34  $i_{\alpha}, i_{\beta}$  Of The Pmsm At 750 Rpm I.E. Current In The Stator At 50 Hz
- 5.35  $\hat{i}_{\alpha}, \hat{i}_{\beta}$  Of The Pmsm At 750 Rpm I.E. Current In The Stator At 50 Hz
- 5.36  $\widehat{e}_{\alpha}, \widehat{e}_{\beta}$  Of The Pmsm At 750 Rpm I.E. Current In The Stator At 50 Hz
- 5.37  $i_{\alpha}, i_{\beta}$  Of The Pmsm At 400 Rpm I.E. Current In The Stator At 26.66 Hz
- 5.38  $\hat{i}_{\alpha}, \hat{i}_{\beta}$  Of The Pmsm At 400 Rpm I.E. Current In The Stator At 26.66 Hz
- 5.39  $\widehat{e}_{\alpha}, \widehat{e}_{\beta}$  Of The Pmsm At 400 Rpm I.E. Current In The Stator At 26.66 Hz
- 6.1 Scheme of Model Adaptive Reference System
- 6.2 Rotor Velocity
- 6.3 Electromagnetic Torque
- 6.4 Iq Current

6.5	Id Current
6.6	Rotor Angle
6.7	Rotor Angle Error
6.8	Electromagnetic Torque
6.9	Rotor Velocity
6.10	Iq Current
6.11	Rotor Angle
6.12	Estimated Rotor Angle Error

## **LIST OF TABLES**

TABLE 1 : Parameters Of Pmsm Modelled In Simulink

TABLE 2: Comparison of different sensorless techniques

## ABBREVIATION

PI	Proportional Integral
MPC	Model Predictive Control
SMC	Sliding Mode Control
SMO	Sliding Mode Observer
VSI	Voltage Source Inverter
SPWM	Sinosoidal pulse width modulator
SVPWM	State Vector Pulse Width Modulation
EMF	Electro Motive Force
MMF	Magneto Motive Force
V	Voltage
A	Ampere
AC	Alternating Current
DC	Direct Current
BLDC	Brushless Dc
PMSM	Permanent Magnet Synchronus Motor
IM	Induction Motor
FOC	Field Orient Control
DTC	Direct Torque Control
EKF	Extended Kalman Filter
MARS	Model Adaptive Reference Syaytem
mH	Milli Henry
kw	Kilowatt
Nm	Newton Meter
Wb	Webers
lpf	Low pass filter

PWM

Pulse Width Modulation

EV

Electric Vehicle

IPMSM

Interior Permanent Magnet Synchronous Motor



## LIST OF SYMBOLS

$i_a$	Armature Current
$u_a$	Armature Voltage
$\Lambda_a$	Stator Flux Linkage
$e_a$	Back Emf
$R$	Stator Resistance
$L_S$	Stator Inductance
$u_d$	Stator Voltage In D Axis
$u_q$	Stator Voltage In Q Axis
$\omega$	Rotor Electrical Velocity
$P$	Output Power
$T$	Developed Torque
$i_d$	Stator Current In D Axis
$i_q$	Stator Current In Q Axis
$\Lambda_d$	Stator D Axis Flux Linkage
$\Lambda_q$	Stator Q Axis Flux Linkage
$\Lambda_{PM}$	Rotor Permanent Magnet Flux
$\omega_e$	Rotor Electrical Velocity

$T_L$	Load Torque
$\omega_m$	Rotor Mechanical Velocity
$p$	Number Of Poles
$L_d$	Stator Direct Axis Inductance
$L_q$	Stator Quadrature Axis Inductance
$J$	Motor Inertia Constant
$\hat{i}_\alpha$	Estimated Alpha Axis Stator Current
$\hat{i}_\beta$	Estimated Beta Axis Stator Current
$i_\alpha$	Alpha Axis Stator Current
$i_\beta$	Beta Axis Stator Current
$R_S$	Stator Resistance
$\varphi_f$	Stator Flux Linkage
$\omega_r$	Rotor Velocity
$e_\alpha$	Alpha Axis Back Emf
$e_\beta$	Beta Axis Back Emf
$\theta$	Rotor Electrical Angle
$U^*$	Three-Phase Sinusoidal Stator Voltage Vector
$s$	Laplace Coefficient

$K_i$	Integral Constant
$K_p$	Proportionality Constant
$V$	Voltage
$\omega_{cutoff}$	Filter Cut Off Frequency
$\theta$	Rotor Electrical Angle
$\hat{\theta}$	Estimated Electrical Rotor Angle
$B$	Viscous Friction Coefficient

# Chapter 1

## INTRODUCTION

### 1.1. INTRODUCTION

AC electrical motors are popularly used in industry. AC motors are used in washing machines, industrial cranes and transportation vehicles (like trains or cars) etc.[1]. AC motors are classified into induction and synchronous motor [1]. The difference between two motors is that in induction motor, current is induced in the rotor windings due the relative motion between the rotor winding and stator magnetic field. While in synchronous motors, there is no relative motion between the rotor winding and stator magnetic field. The rotor magnetic field is generated by injecting current in the rotor winding or by using permanent magnet. Induction motors are more popular in industry because they are smaller in size, robust and cheap [2]. But Induction motor are difficult to control due to complex and non linear behaviour of motor. However, Permanent Magnet Synchronous Motors (PMSM) are gaining popularity due its high power/mass ratio and higher Efficiency. The main drawback of PMSM is that, it is more expensive due to which it is mostly used for high performance applications [3]. Brushless DC (BLDC) motor are similar to PMSM in construction as they have permanent magnets in the rotor and require alternating stator currents [4]. The main difference lies in the back emf of the two motors as the back emf of BLDC is trapezoidal whereas the back emf of PMSM is sinusoidal ,due to which the torque of PMSM has reduced ripple. This gives a difference in the operating requirements of the two motors.

Field Oriented Control (FOC) is used to separately control the flux and torque of motor[5]. The three stator currents, represented in a three coordinate reference frame(abc) are transformed into a rotating two coordinate reference frame(dq).The exact position of the rotor is required for the transformation. The two components are controlled independently. The control output is motor voltage command which is transformed into rotating frame ( $\alpha$ - $\beta$ ) and fed to SVPWM inverter to produce the sinusoidal voltages that is applied to the motor.

For the field oriented control, rotor angle is sensed by electromagnetic resolvers or by using incremental or absolute encoders. Electromagnetic resolvers are popular for measuring the rotor position because of their rugged construction and higher operating temperature. However, sensors require extra space and mounting on the shaft of the motor .This decreases the reliability of the system, increases the cost and require additional maintenance, the sensor can be replaced by technique that mathematically estimates the speed or position of the rotor. This is called sensorless control [2], [3].

According to [17], the main objectives of sensorless drive control are:

- 1) Increase in mechanical robustness
- 2) Reducing cost and hardware complexity
- 3) High reliable operation in hostile environment
- 4) Low maintenance requirements
- 5) Increased noise immunity
- 6) No affect on machine inertia

## 1.2. Background

According to [12] “in 2018, 93 per cent of all passenger EVs sold globally used PMSMs”. Permanent magnet synchronous motors are up to 15 per cent more efficient than induction motors and are the most power-dense type of traction motor commercially available. Despite being costly, they are economically attractive because increasing the battery capacity by 5 % for most efficient induction motor increases the powertrain cost more than double cost of PMSM motor.

Vector control of motor is more popular method due to increased efficiency and output power quality. Sensors are required for the vector control. Hence this decreases the reliability of the motor. Hence, more focus is on the sensor less techniques to increase the reliability of the powertrain.

## 1.3. Problem Definition

A lot of literature is available for sensorless techniques for PMSM. But the comparison between the different sensorless techniques is not widely available in the literature. This project compares the different sensorless techniques for PMSM. This project simulates the different sensorless techniques and evaluate the best for the above application.

## 1.4 Scope

The Surface mounted PMSM (SPMSM) is being considered due to its structural stability in high speed application. The sensorless techniques which are applicable to SPMSM are applicable are considered and the rest are discarded. The sensorless methods which are applicable to Field oriented control of motor are only considered. There are two types of estimator available, low speed estimators and high speed estimators, both are considered. Speed estimator and rotor position estimators are considered but they can be derived from each other.

Only two techniques are evaluated and simulated later to take into account the time frame of this project. One techniques is simulated and improved further to obtain better results.

## 1.5 Methodology

In the literature study the different sensorless techniques are discussed and compared. They are discussed and compared on the basis of their low and high speed applications, computational complexity and robustness against parameter variation. Sensored control of PMSM is simulated. Only two of the sensorless techniques are considered and simulated further. Only one techniques is further improved to obtain better result. The Two test cases are modelled on Simulink and the chosen two sensorless techniques are tested on following two test cases.

In this project speed control of PMSM is implemented in sensored mode and sensorless mode. The PMSM motor with parameter in table 1.1 is mathematical modelled in Simulink. Two test cases are tested on simulated in this project.

1. The speed reference is changed from 400 rpm to 750 rpm with rated load torque of 20 Nm
2. The torque load is changed from 20 Nm to 10 Nm with rated speed of 750 rpm

These test cased are satisfactorily test the performance of motor under the various loading conditions. Simulation should mirror the performance of the drive in real world conditions.

Rated power	9.4 kw
Stator Resistance( $R_s$ )	0.203 $\Omega$
Pole pairs( $p$ )	4
Inductance( $L_d=L_q$ )	2.10 mH
Inertia( $J$ )	0.0048 kg.m <sup>2</sup>
Permanent Magnet flux	0.123 Wb
Rated torque	20 Nm

TABLE 1 : Parameters Of Pmsm Modelled In Simulink

## 1.6 Content

In the second chapter, several research paper are analysed and various techniques are discussed and compared. In the third chapter, theory associated with various components in FOC of PMSM is explained .In the Fourth chapter, FOC of motor with rotor position information from sensors is modelled in Simulink. The PI is tuned to improve the performance. In the fifth chapter, FOC with SMO for sensorless control is modelled in Simulink. In the sixth chapter, FOC with MRAS for sensorless control is modelled in Simulink. In the seventh chapter, conclusion are drawn and future work is discussed.

## Chapter 2

### LITERATURE SURVEY

#### 2.1. LITERATURE SURVEY

Two different type of sensorless technique are proposed in literature, one is saliency tracking method and emf model based methods. Saliency tracking method is suitable for low and medium speed application whereas Emf model based method is suitable for medium and high applications. Saliency tracking method require high frequency signal injection in the motor which induces acoustic noise and ripples in the torque due to which the applications are limited.

Emf model based method have limitation at low speed application as induced back emf is less at low speed. Due to which a starting method is required.

Popular model based methods are:

- A. Sliding Mode Observer
- B. Model reference adaptive System
- C. Extended Kalman Filter
- D. Flux Estimation Method

#### 2.2. SLIDING MODE OBSERVER

Sliding mode control is a type of variable structure control system in which control is a function of system state that switches at infinite (theoretically) frequency[17]. It does not depend upon structures with different properties and different switching. The function switches discretely from one state to another state at high frequency. The system is forced to slide on sliding surface and this motion is called sliding mode. The convergence of the smo to the sliding surface is verified by lyapunov theorem.

Sliding mode observer is used to estimate the back emf of the PMSM, which in turn to estimate the rotor angle and rotor speed. Back emf is the function of rotor electric angle and speed. Sliding mode observer is robust against parameter variation of system. Although, Chattering is a major disadvantage of sliding mode observer. Literature [1,2,3] uses different switching function, in order to reduce chattering. Various different techniques are used to reduce the chattering effect. In [1], proposes sliding mode observer for PMSM with washing machine application. Instead of signum function, saturation function is proposed in order to reduce the chattering effect. A novel variable linearized gain  $l$  is used to improve the performance of the system at low speed. In terms of performance, the observer is suitable for the application requiring wide speed range, including



the flux-weakening region. Although the presence of low pass filter demerits the dynamic performance of system. Various phase compensation techniques are described in literature [14]. Uses [13] the lookup table to calculate the phase compensation required which uses a significant amount of memory space due to which extra memory is required. Some uses variable phase compensation which compensates according to the rotor velocity and the filter cut-off frequency. Since, the speed is also estimated and some inherent noise, hence there can be large fluctuation in phase compensation, therefore, this method is also not preferred. [14] Uses the low pass filter with variable cutoff frequency which is a function of rotor velocity which constant compensation, this technique is preferred at low speed and at high speed. Various speed estimation methods discussed in literature [1][2][3]. In [2] simply the differentiation of rotor angle is done to derive the rotor speed but this method is not preferred due to inherent chattering in the rotor angle which introduces error in the system. PLL [1] and back emf based observer [3] are also used to estimate the rotor speed, but this affect dynamic response of the system. [] uses the back emf to estimate the speed. [2] paper proposes SMO with sigmoid function with variable boundary layer ,so as to eliminate the lpf in the system. The stator resistance is estimated in the SMO, so as to take account of variation of stator resistance with time and improve the performance. The observer gain is proposed to be a linear function of rotor velocity, so as to reduce the chattering. Although the chattering is reduced but is present significantly in the system. There are issues with the performance of the drive at low speed.[3] Paper proposes novel SMO for the PMSM . A back EMF observer is proposed which is applied after back emf signal are obtained .This paper claims not in this way, lpf and phase compensation module are eliminated but also the static and dynamic performance is improved. The significant reduction in chattering is also obtained. [4] Proposes SMO with new hyperbolic function with proper boundary layer so as to significantly reduce the chattering effect. The proposed SMO simplifies the system with the reduction in the lpf and phase compensation module. But the variable nature of observer gain increases the complexity.

### 2.3. Model Reference Adaptive System

Model Reference Adaptive System(MRAS) consist of two model : one is the reference model and other is adaptive model. Reference model is the same model of the system having performance as required by the adjustable model. Reference model and adaptive model are connected in parallel having the same input  $r(t)$ . The output from the two model are compared and error  $e(t)$  is obtained . The error is fed to the adaptive mechanism which varies the state variable of the adjustable model such that the error  $e(t)$  converges to zero. The asymptotic stability of the model reference adaptive is guaranteed by lyapunov stability theorem and popov hyper stability theorem

The motor model is taken same as the reference model which took into the account parameter deviation of the system with time. The state variable such as current or power are taken as output from the reference model and adjustable model and error  $e(t)$  is obtained. By using adaptive

mechanism calculates the speed  $\omega_r$ , the estimated speed is fed to the adaptive mechanism which in turn estimate the stator current

Traditionally PI controller is used in adaption mechanism because of easy implementation but better result also obtained with Ann.

MRAS is popular because of simple implementation and wide speed operation .The major disadvantage of MRAS is dependence on parameters of the motor as MRAS heavily depends on system mathematical model. This can be overcome by taking the motor as the reference model[2][3]. However, in the [1] this problem is taken care by estimating the rotor parameters in real time. [5]This paper proposes the sensorless control of PMSM with MRAS multiparamter estimation based on the feedforward voltage estimation. This MRAS model removes the dependence on the parameter of motors by estimating the stator resistance, rotor flux linkage magnitude and stator inductance is set to its nominal value.[6,7]. The paper proposes the sensorless control with PMSM having PI as adaptive mechanism.

## 2.4. Extended Kalman Filter

Kalman filter is defined as for linear system , in extended kalman filter the system is linearized around operating point by Taylor theorem ,higher order terms of Taylor expression are omitted.

Kalman filter is a recursive method for optimal state estimation. It is used for parameter estimation of a non-linear dynamic system in real-time by using noisy monitored signals that are distributed by random noise [17]. This assumes that the measurement noise and disturbance noise are uncorrelated. It consist of two step prediction step and correction step. The Kalman gain is updated in each loop.

EKF is used to calculate the real time estimation of rotor angle and speed. The main aim of extended kalman filter is to estimate the unmeasured state i.e. rotor angle and velocity by using measurable state variable i.e. motor terminal voltage and current. However, the extended kalman filter implementation is computationally expensive and accuracy is dependent on rotor parameters. The design and the tuning of the covariance matrices that appear in the EKF equations [8][9][10][11] is time consuming and convergence is always not guaranteed.

## 2.5. Flux Observer Method

Flux observer method is defined for open loop and closed loop .In open loop the rotor flux linkage are estimated using the mathematical model of motor ,which in turn are used to calculate the rotor angle. This possess another problem as low speed, voltage due to rotor resistance is more than the voltage applied at the motor terminals.

This method is simple. But this method depends on the rotor motor equations for flux estimation due to which it depend on the motor parameters. Some extra compensation is required due to which its simplicity is lost.

## 2.6. Discussion

The above methods are compared on the basis of estimation accuracy, processor requirement, ability to use on different motor, rotor resistance estimation requirement and their parameter variation sensitivity.

	Flux based	SMO	EKF	MRAS
Estimation Accuracy	Average	Better	Good	better
Processor requirement	low	low	high	low
Retuning Ability	Good	Good	Bad	Good
Resistance Estimation requirement	May be	No	May be	Yes
Parameter variation sensitivity	Bad	Can be improved	Decent	Decent

TABLE 2: Comparison of different sensorless techniques

Estimation accuracy denotes how much the estimated value is near the real value. Ability to converge to the real value is a necessary requirement for any estimator. EKF has good estimation accuracy which also denotes its computation requirement. SMO has high frequency signal which can be filtered out. All the above estimator perform fairly in the estimation accuracy requirement.

The computational requirement for the estimator should be low as low end microprocessor can be used and decrease the cost of the system. The EKF has to obtain inverse of matrix and many matrix multiplication in one sample time, therefore it has high computational load. High end processor is required for EKF estimator. The SMO require the computation of back emf and the MRAS has to PI control for the estimation of position and speed respectively. These processes do not require high computation demand and can be easily done by low end processor.

The ability of the estimator to retune it for different motor is also considered. With the change in the parameters of the motor, the tuning of the estimator is also carried out. The SMO has to change in only one parameter, so as to satisfy the stability condition. The MRAS has to only tune one PI. Whereas for EKF, three different have to be retuned.

When the motor heat up, the armature resistance changes. Since these estimation techniques depend on the motor model, so some resistance estimation is required. SMO is mostly remain

unaffected by resistance but it may affect dynamic performance. MRAS requires the rotor resistance estimation.

From the above discussion it can be deduced that SMO and MRAS satisfy our operational requirement. Hence they are further mathematical modelled in Simulink.

# Chapter 3

## Theory

### 3.1. Permanent Magnet Synchronous Machine

This section describe the equation used to model the PMSM in the Simulink. The Clark and Parke transformation are also described. The PMSM motor are modelled in abc ,  $\alpha$ - $\beta$  and dq frame.

#### 3.1.1. PMSM model in abc frame

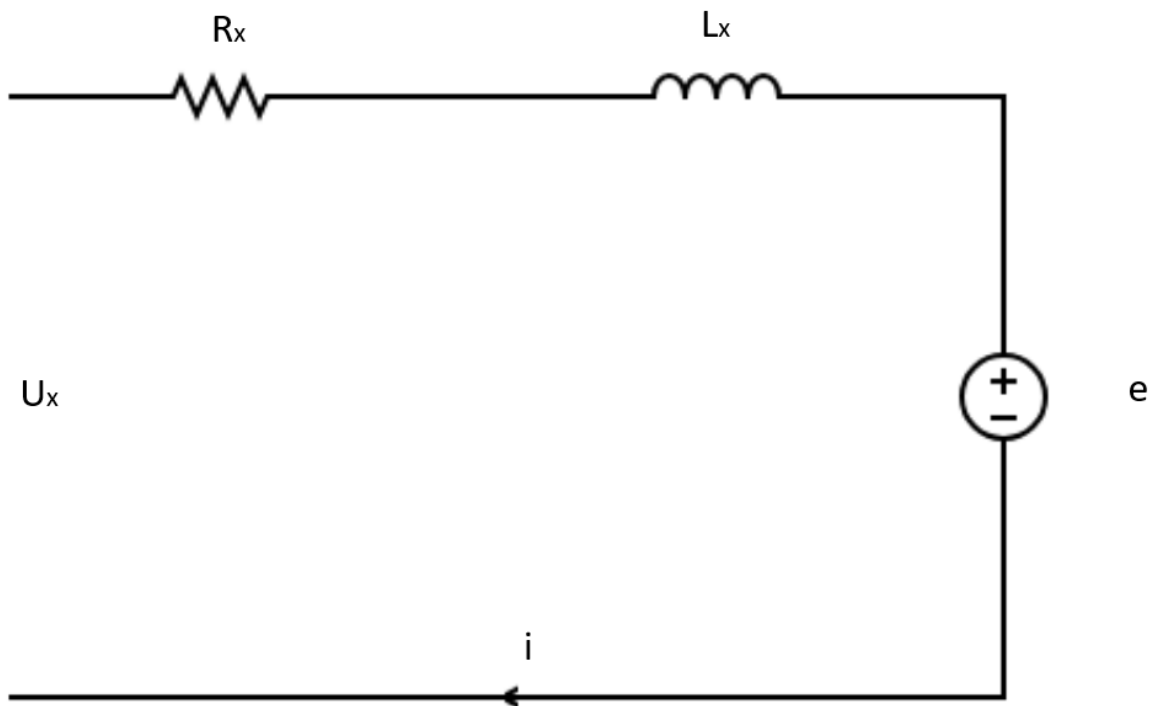


Figure 3.1

Equivalent circuit of a motor in dq0 phase

In abc frame, each phase is equally distributed in plane with 120 degree phase shift. The equivalent circuit of one phase of PMSM with a non-salient rotor is shown in Figure 3.1.

From Figure 3.1, the voltage equations for a PMSM are given by Equation 3.1

$$\begin{aligned}
u_a &= Ri_a + \frac{d\Lambda_a}{dt} = Ri_a + L_S \frac{di_a}{dt} + e_a \\
u_b &= Ri_b + \frac{d\Lambda_b}{dt} = Ri_b + L_S \frac{di_b}{dt} + e_b \\
u_c &= Ri_c + \frac{d\Lambda_c}{dt} = Ri_c + L_S \frac{di_c}{dt} + e_c
\end{aligned} \tag{3.1}$$

Where,  $\Lambda_a$ ,  $\Lambda_b$  and  $\Lambda_c$  are the instantaneous flux linkage to the stator  $u_a$ ,  $u_b$  and  $u_c$  are the instantaneous voltage across the stator terminal.  $i_a$ ,  $i_b$  and  $i_c$  are the instantaneous stator current.

### 3.1.2. PMSM model in $\alpha$ - $\beta$ frame

The abc frame is transformed to two orthogonal frame which are in the abc frame of reference. The transformation from abc to  $\alpha$ - $\beta$  frame is given by Clarke transformation:

$$\begin{bmatrix} f_\alpha \\ f_\beta \end{bmatrix} = \sqrt{\frac{2}{3}} \begin{bmatrix} 1 & -\frac{1}{2} & -\frac{1}{2} \\ 0 & \frac{\sqrt{3}}{2} & \frac{\sqrt{3}}{2} \end{bmatrix} \begin{bmatrix} f_a \\ f_b \\ f_c \end{bmatrix}$$

The mathematical model of PMSM alpha beta frame is given by following equations:

$$\begin{aligned}
L_S \left( \frac{d\hat{i}_\alpha}{dt} \right) &= -R_S i_\alpha - e_\alpha + u_\alpha \\
L_S \left( \frac{d\hat{i}_\beta}{dt} \right) &= -R_S i_\beta - e_\beta + u_\beta
\end{aligned} \tag{3.2}$$

$i_\alpha$ ,  $i_\beta$ ,  $e_\alpha$ ,  $e_\beta$ ,  $u_\alpha$ ,  $u_\beta$  are the phase currents, back emf and phase voltages in alpha-beta reference frame.  $L_S$  is the stator inductance and  $R_S$  is the stator resistance.

### 3.1.3. PMSM model in dq0 frame

The motor equation are transformed from abc frame to dq frame by parks transformation

$$\begin{bmatrix} f_d \\ f_q \\ f_o \end{bmatrix} = \frac{2}{3} \begin{bmatrix} \cos(\theta) & \cos\left(\theta - \frac{2\pi}{3}\right) & \cos\left(\theta + \frac{2\pi}{3}\right) \\ \sin(\theta) & \sin\left(\theta - \frac{2\pi}{3}\right) & \sin\left(\theta + \frac{2\pi}{3}\right) \\ \frac{1}{2} & \frac{1}{2} & \frac{1}{2} \end{bmatrix} \begin{bmatrix} f_a \\ f_b \\ f_c \end{bmatrix} \quad (3.3)$$

The dq0 frame is stationary with respect to rotor frame. This frame of reference is used to model the PMSM in Simulink. All the AC quantities are converted to DC values which are easier to control. Since the three phase in the motor are balanced, the last row,  $f_o$  is equal to zero.

Since the dc values can be easily controlled by PI control, this is preferred method for controlling the motor. Equation below are the motor voltage equations in dq0 reference frame after transformation.

$$u_d = Ri_d + \frac{d\Lambda_d}{dt} - \omega\Lambda_q \quad (3.4)$$

$$u_q = Ri_q + \frac{d\Lambda_q}{dt} + \omega\Lambda_d \quad (3.5)$$

Where

$$\Lambda_d = L_d i_d + \Lambda_{PM} \quad (3.6)$$

$$\Lambda_q = L_q i_q \quad (3.7)$$

Where  $\Lambda_d$ ,  $\Lambda_q$  are d and q axis flux linkage,  $L_d$  and  $L_q$  are direct axis and quadrature axis inductance,  $\omega$  is the electrical angular velocity and  $\Lambda_{PM}$  is the permanent magnet flux.

Equation 3.8 describes the instantaneous power in a three phase motor. power in dq frame is calculated by equation 3.9 .

$$P = u_a i_a + u_b i_b + u_c i_c \quad (3.8)$$

$$P = \frac{3}{2} (u_d i_d + u_q i_q) \quad (3.9)$$

The electrical torque produced by the motor is given by equation 3.10 and 3.11, There is cross coupling between the d and q axis flux linkage and current .This is not preferred. Since we are using a non- salient pole motor i.e.  $L_d = L_q$ , hence the first term in the equation is null and also we will be using the vector control where  $I_d = 0$ , therefore the first term is equal to zero. Therefore the torque will be only directly proportional to  $I_q$  current and there will be no coupling between the d and q axis.

$$T = \frac{3}{2} p (\Lambda_d i_q - \Lambda_q i_d) \quad (3.10)$$

$$T = \frac{3}{2} p ((L_d - L_q) i_d i_q + \Lambda_{PM} i_q) \quad (3.11)$$

The relationship between the electrical angular velocity and the mechanical angular velocity is shown in equation 3.12 For a synchronous machine the relationship between the mechanical angular velocity and the electrical angular velocity is described by Equation 2.11. The motor mechanical dynamic equilibrium is shown in equation 3.13.

$$\omega_e = p\omega_m \quad (3.12)$$

$$T = J \frac{d\omega_m}{dt} + B\omega_m + T_L \quad (3.13)$$

Where  $\omega_e$  is the rotor electrical angular velocity,  $\omega_m$  is the rotor mechanical angular velocity,  $p$  is the number of pole pairs,  $T$  is the electrical torque produced by the motor,  $T_L$  is the load torque,  $J$  is the inertia constant and  $B$  is the viscosity friction coefficient.



### 3.2. Field Oriented Control

With field orient control, the superior control of dc motor is obtained in ac motor. In field oriented control, the motor current is controlled in dq frame, instead of abc frame, due to which, the electrical current of motor in dq frame is independent of the rotor position. The DC currents are easier to control than AC current. The d component of the current controls the flux and the q component controls the torque [5], [9]. The FOC can thus manage to control both flux and torque by controlling the currents in d and q coordinates separately. . Proportional Integral Controllers, PI, are used to regulate the d and q output current components with reference currents in order to control the speed and torque. A FOC control scheme applied on the PMSM is illustrated in Figure 2.4

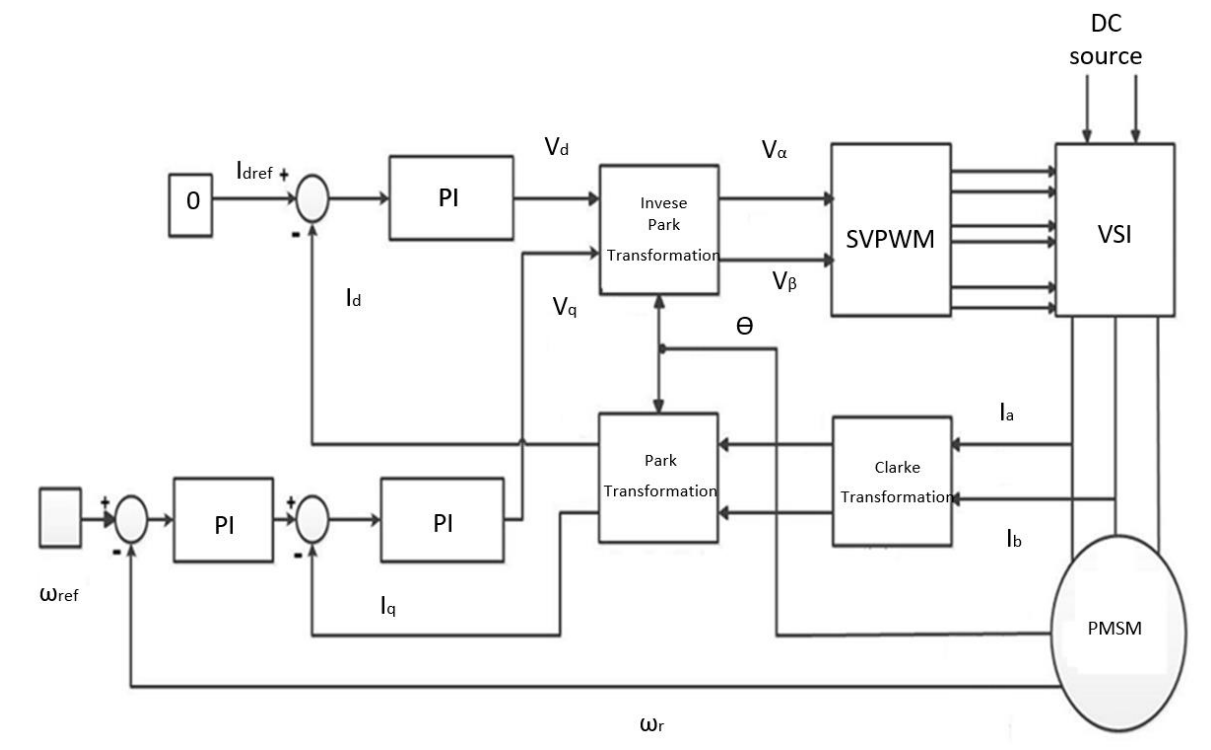


Figure 3.2

Field Oriented Control Of PMSM

### 3.3. Space Vector Modulation

Sinusoidal SPWM and space vector modulation (SVPWM) are popular PWM technique for VSI. SVPWM is as part of FOC to generate rotating vector in motor The SVPWM improves the DC link utilization by 15.15%.

There are eight switch combination possible in a three phase inverter. Two of them corresponds to the zero output voltage and other six apply non zero output voltage. In Figure 3.3 the phase voltage space vectors are represented. The zero vectors are at the centre of figure and have zero magnitude and they are used to insert dead time in the inverter. These six vectors divides the plane into six sectors spaced 60 degrees. The maximum amplitude voltage that the inverter can produced is  $2/3U_{dc}$ . The centre of the hexagon corresponds to zero vector.

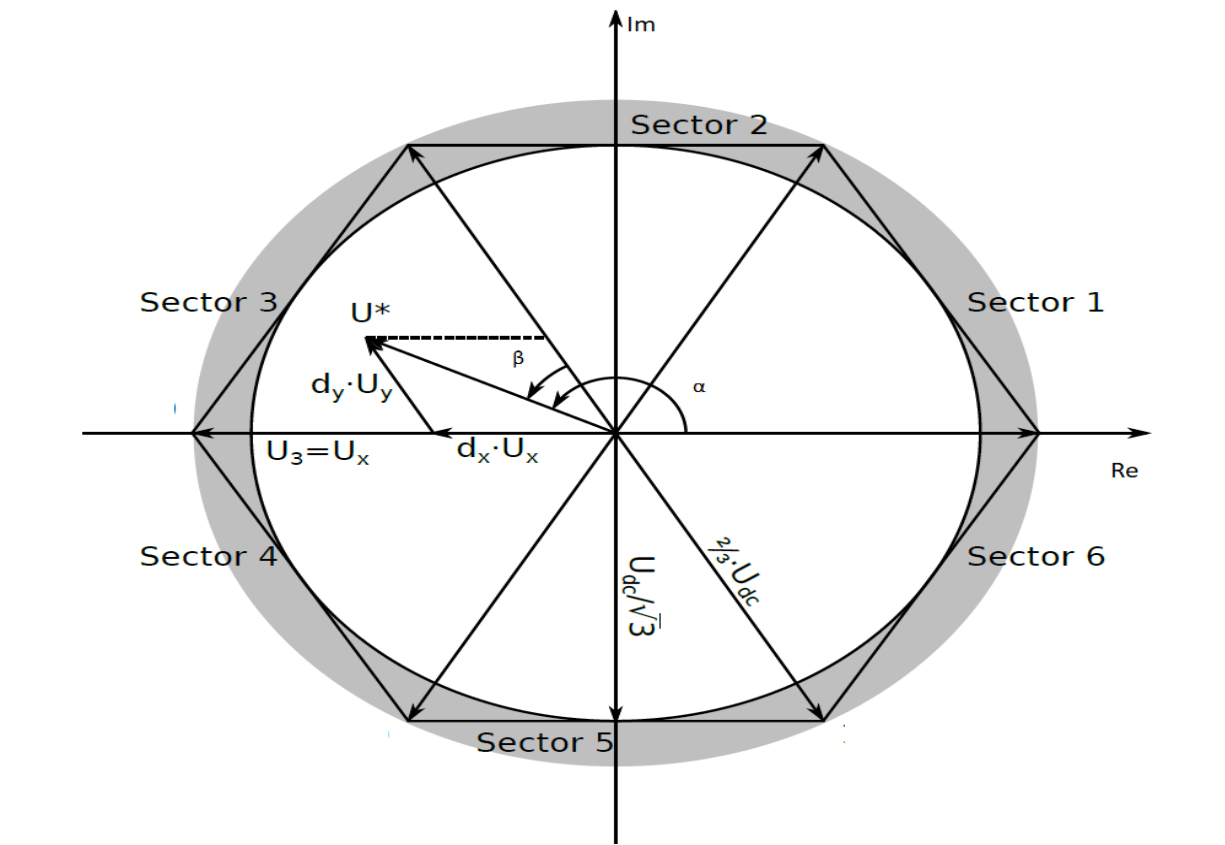


Figure 3.3

SVPWM

$U^*$  is the voltage vector that the inverter has to reproduce in output. The maximum magnitude voltage that can be reproduced is  $2/3U_{dc}$ .

As shown in figure 3.3,  $U^*$  voltage vector is placed in one of the sector. The voltage vector  $U^*$  can be reproduced in the output by using two of the active vectors with the one of the zero vector or both of the zero vectors with the switching time defined accordingly. The dead duty is mostly distributed over both the zero vectors to avoid the switching fatigue. For a general case, the vector  $U^*$  can be resolved into two active vectors  $U_x$  and  $U_y$ , as in figure 3.3, their corresponding duty cycles are  $d_x$  and  $d_y$  which can be obtained as follows:

$$U^* = |U^*| \begin{pmatrix} \cos \beta \\ \sin \beta \end{pmatrix} = d_x |U_x^*| \begin{pmatrix} 1 \\ 0 \end{pmatrix} + d_y |U_y^*| \begin{pmatrix} \cos \frac{\pi}{3} \\ \sin \frac{\pi}{3} \end{pmatrix} \quad (3.14)$$

$$= d_x \frac{2}{3} |U_{dc}| \begin{pmatrix} 1 \\ 0 \end{pmatrix} + d_y \frac{2}{3} |U_{dc}| \begin{pmatrix} \cos \frac{\pi}{3} \\ \sin \frac{\pi}{3} \end{pmatrix} \quad (3.15)$$

Where,

$$d_x = \sqrt{3} \frac{|U^*|}{|U_{dc}|} \sin \left( \frac{\pi}{3} - \beta \right) \quad (3.16)$$

$$d_y = \sqrt{3} \frac{|U^*|}{|U_{dc}|} \sin(\beta) \quad (3.17)$$

The duty cycle  $d_o$ , corresponds with the zero vectors and is given by

$$d_o = 1 - d_x - d_y \quad (3.18)$$

# Chapter 4

## Sensored control

### 4.1. Sensored control

In Sensored control the resolver and encoders are used to detect the position of rotor and to estimate the speed for the field oriented control of motor. Speed control of the motor is implemented in this project. Three PI control are used to control the motor in closed loop. One PI generates the  $V_d$  by comparing the reference  $I_d$  and actual  $I_d$  of the motor calculated after the Clarke and Park transformation and second PI generates the  $V_q$  by comparing the reference  $I_q$  and  $I_q$  of the motor. Third PI generates the  $I_q$  reference by comparing the speed reference and the speed of the motor.

### 4.2. PI control design

The model equation in dq0 in terms of the Laplace transform variable  $s$  is given in equation 3.19 and 3.20

$$u_d(s) = (sL_d + R)i_d(s) - \omega L_q i_q(s) \quad (4.1)$$

$$u_q(s) = (sL_q + R)i_q(s) - \omega(L_d i_d(s) + \Lambda_{PM}) \quad (4.2)$$

As, it can be seen that there is cross coupling between the d axis and q axis terms in the equation. Therefore, the equations are non-linear. PI can only control the linear system. Hence, the cross coupling term are required to be eliminated. An external disturbance is added into the control loop as shown in Figure 4.1

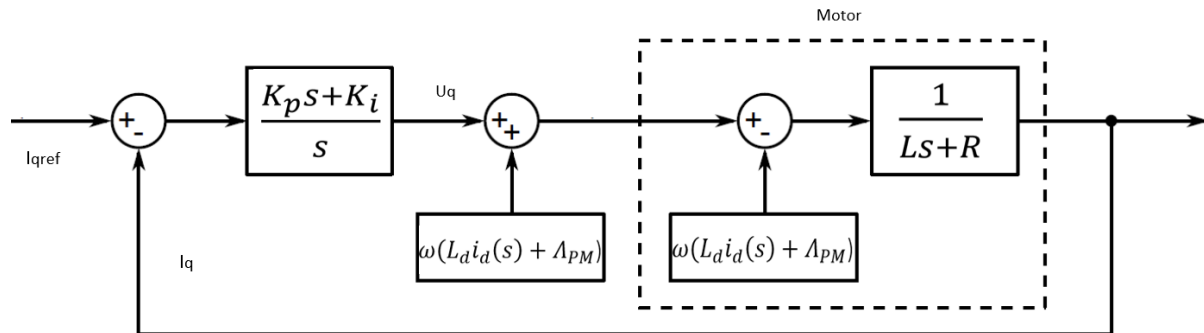


Figure 4.1

$I_q$  current loop with an external disturbance

This external disturbance has same value but opposite sign of the back-EMF term. Same principle can be applied for decoupling in d axis equation.

The system can be simplified to a second order system as shown in Figure 4. It can be see that, for a non-salient pole machine where  $L_q=L_d$ ., the. current control loop in both axes would be identical

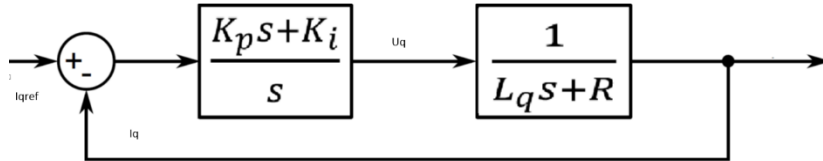


Figure 4.2	Simplified Iq loop
------------	--------------------

For open loop, we have open loop transfer function, we have

$$G_{OL}(s) = \frac{K_p s + K_i}{s} \frac{1}{L_q s + R} \quad (4.3)$$

For close loop, we have

$$G_{CL}(s) = \frac{G_{OL}(s)}{1 + G_{OL}(s)} \quad (4.4)$$

$$G_{CL}(s) = \frac{\frac{K_p}{L}(s + \frac{K_i}{K_p})}{s^2 + s(\frac{R + K_p}{L}) + \frac{K_i}{L}} \quad (4.5)$$

Let,

$$s^2 + s\left(\frac{R + K_p}{L}\right) + \frac{K_i}{L} = (s + C)(s + D) \quad (4.6)$$

Such that

$$(s + C) = \left(s + \frac{K_i}{K_p}\right) \quad (4.7)$$

Thus we have obtains first order transfer function

$$G_{CL}(s) = \frac{\frac{K_p}{L}}{(s+D)} \quad (4.8)$$

We have obtained  $K_p= 8$  and  $K_i= 605$ . Similar procedure is done for  $I_d$  loop PI .

The third PI control for the speed control is used to generate the  $I_q$  reference is tuned using the PI tuner app of the matlab.  $K_p= 0.20$  and  $K_i= 24.6$  are the values obtained for this from PI tuner app. With these value of PI, the field oriented control of motor is modelled in Simulink.

### 4.3 Simulation

In this project speed control of PMSM is implemented in sensed mode . Two test cases are tested on simulated in this project.

1. The speed reference is changed from 0 to 750 rpm with rated load torque of 20 Nm
2. The torque load is changed from 20 Nm to 10 Nm with rated speed of 750 rpm

These test cased are satisfactorily test the performance of motor under the various loading conditions. Simulation should mirror the performance of the drive in real world conditions.

With these tuned values, case 1 is implemented in model.

Peak overshoot of 8.53 % with settling time of 0.029 sec is obtained in speed, when the speed reference is changed from 200 rpm to 750 rpm. Although there is sharp rise in the electromagnetic torque ( $T_e$ ) and  $I_q$  is noticed, because of high acceleration requirement of the rotor, in the transient motion of the motor. This effect also noticed in the  $I_d$  current due to coupling nature of d and q coordinates in the back emf of motor.

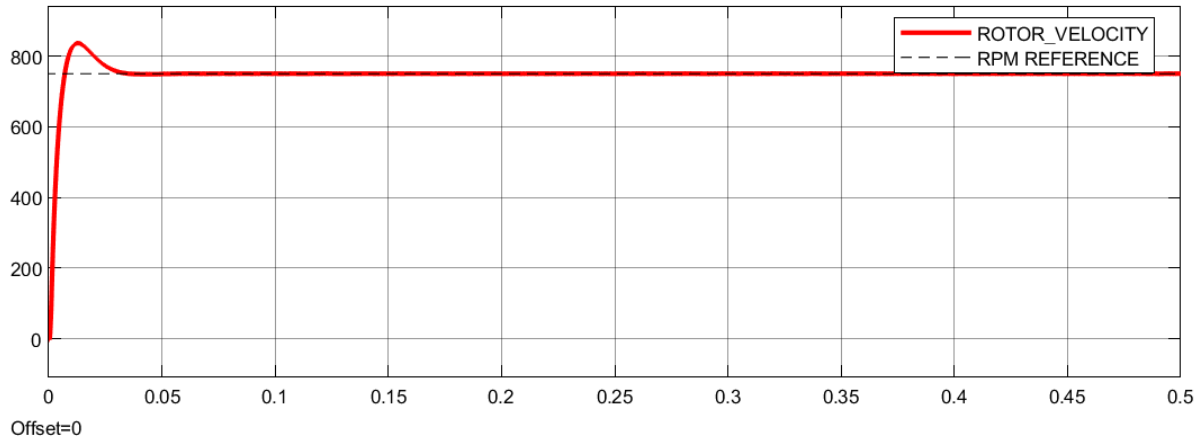


Fig no:4.3 rotor velocity response when speed reference is changed from 0 to 750 rpm

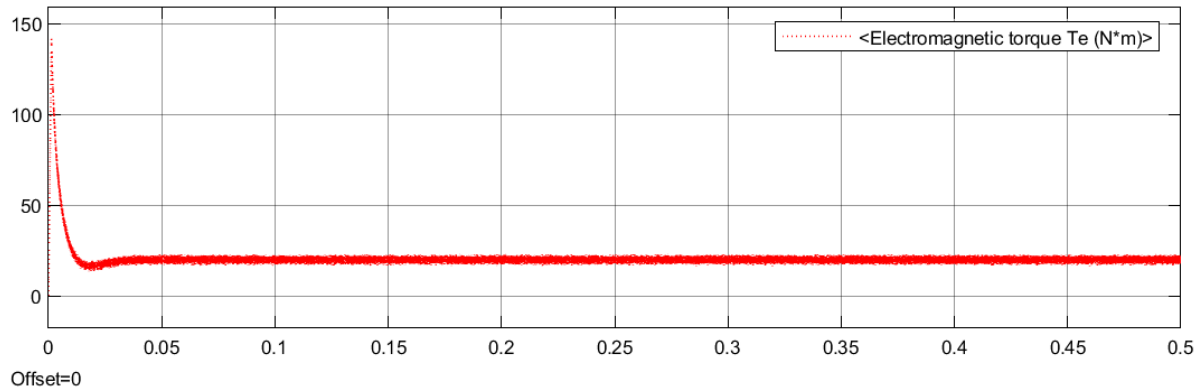


Fig no 4.4 Electromagnetic torque when speed reference is changed from 0 rpm to 750 rpm

Peak in electromagnetic torque is observed in the transient condition due to the acceleration requirement of the rotor.

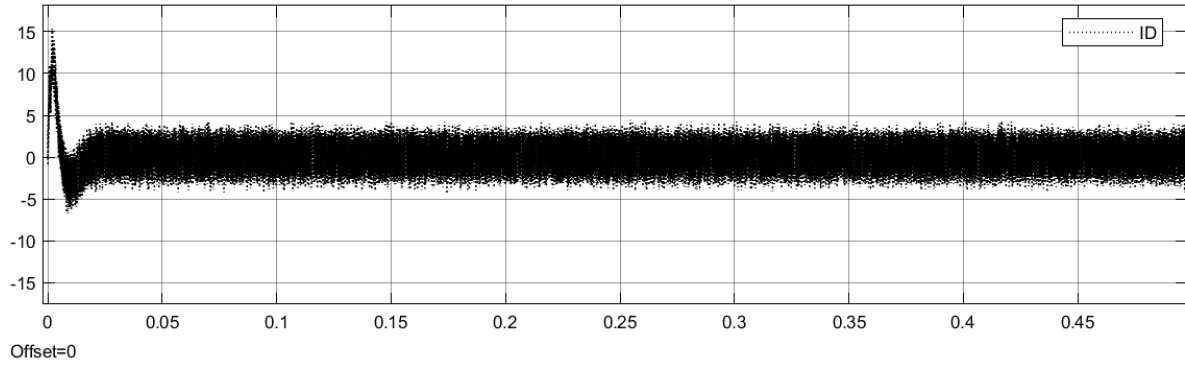


Fig no: 4.5 Id current when speed reference is changed from 0 rpm to 750 rpm

Id current is set reference at 0, although deviation is observed in the Id current when the speed is changed from 200 rpm to 750 rpm.

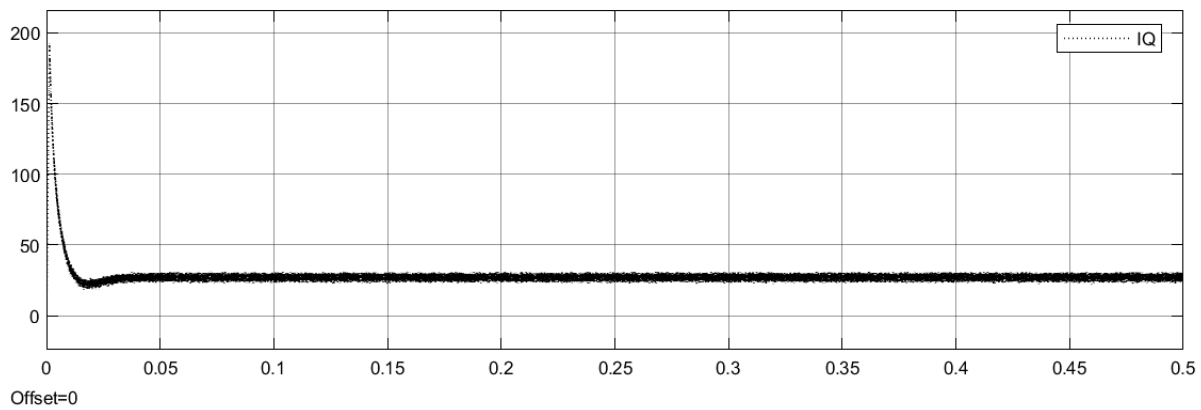


Fig no:4.6 Iq current when speed reference is changed from 0 rpm to 750 rpm for the rated load torque of 20 Nm

Iq current is directly proportional to electromagnetic torque, according to the equation, when the  $I_d = 0$ , In the steady state the Iq current is equal to 27.1 A , when the rated load torque is equal to 20 Nm.



test case 2 is implemented : Torque load is changed from 20 Nm to 10 Nm, slight change in speed is observed in the transient state .

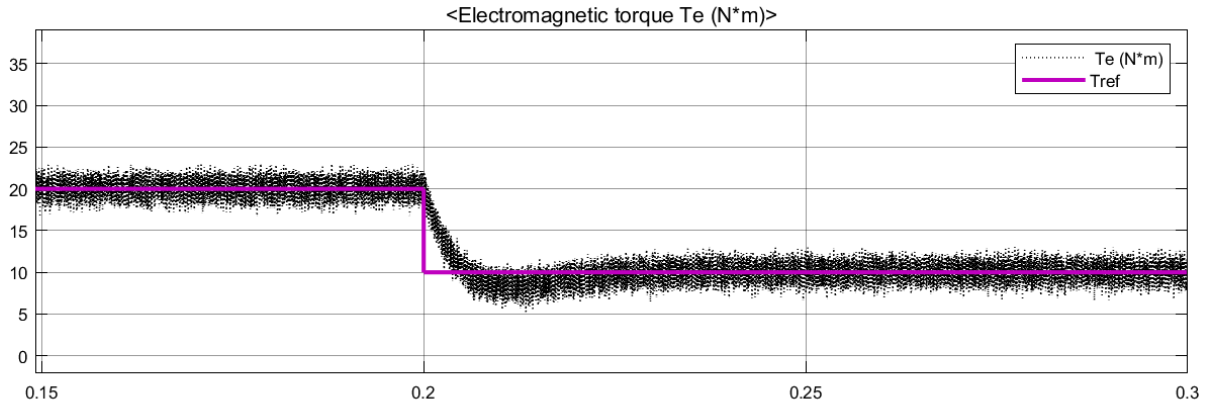
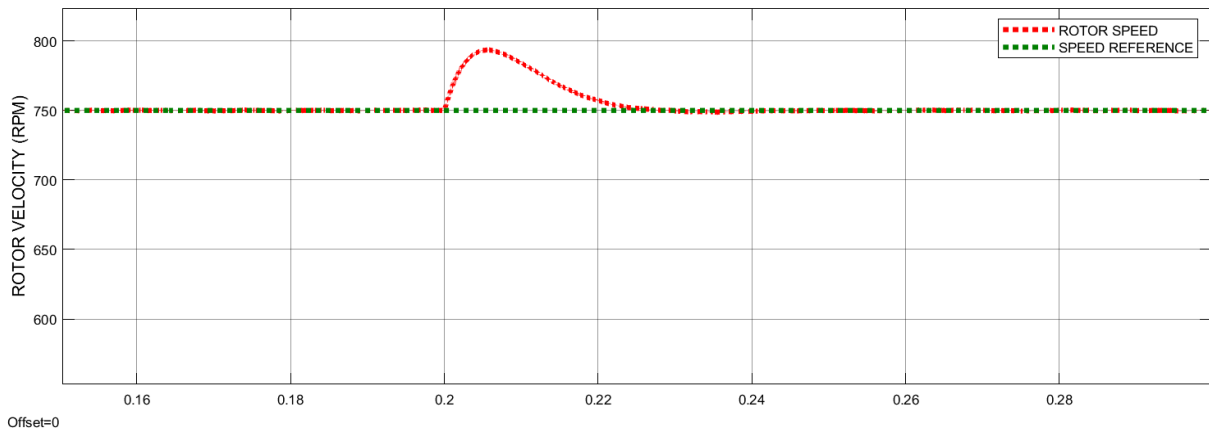
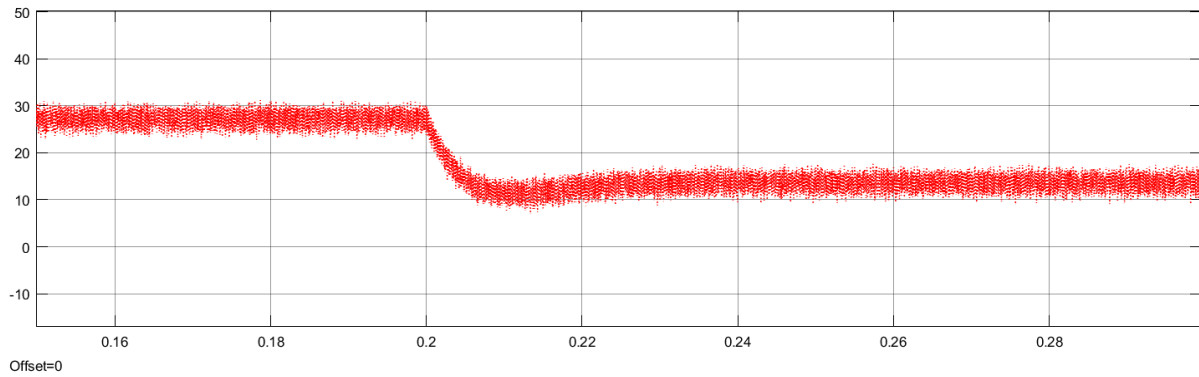


Fig no 4.7 Electromagnetic torque when the torque load is changed from 20 Nm to 10 Nm with rated speed of 750 rpm

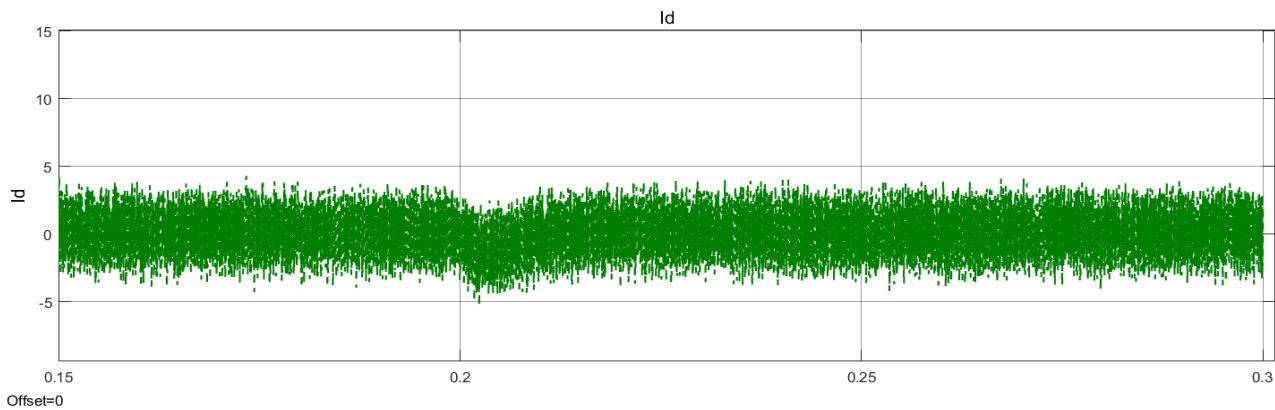


4.8 Rotor Velocity When The Torque Load Is Changed From 20 Nm To 10 Nm With Rated Speed Of 750 Rpm



4.9 Iq Current When The Torque Load Is Changed From 20 Nm To 10 Nm With Rated Speed Of 750 Rpm

Iq current is directly proportional to electromagnetic torque when then  $I_d = 0$ , according to the equation, the same proportionality is noticed in the simulation.



4.10 Id Current When The Torque Load Is Changed From 20 Nm To 10 Nm With Rated Speed Of 750 Rpm

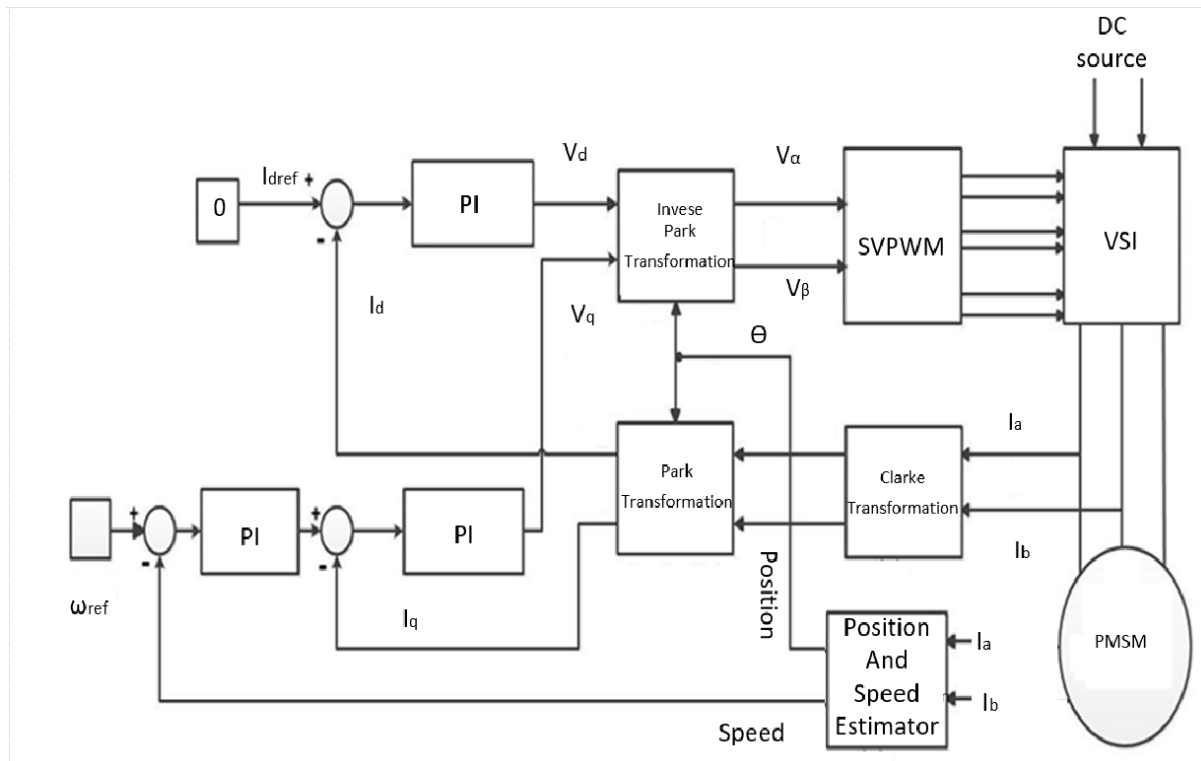
Id current,  $I_d$  reference = 0 , although slight fluctuation is observed due to coupling nature of d and q coordinates.

Since, sensed control is not the primary goal of this project, hence further analysis is not done.

# Chapter 5

## Sensorless Control

### 5.1. Sensorless Control



5.1

Sensorless Control

In a sensorless control, the encoder or resolver is replaced by an state observer that estimates the position and speed of the rotor . The sensorless FOC scheme is illustrated in Figure 4.9.

In this project, sensorless control of PMSM is simulated .Two types of sensorless techniques are implemented in this project

1. Sliding Mode Observer (SMO): Two types of SMO are implemented, one with saturation function and it further improved with a new modified SMO.

2. Model Adaptive Reference System (MRAS): Basic MRAS is implemented is tested under various test conditions.

## 5.2. Sliding Mode Observer(SMO)

SMO are known for their robust nature against the parameter variation. SMO are based on back emf estimation of the PMSM, but at the starting and low speed back emf resolution is low ,hence a starting method is required in the SMO. So in starting open loop v/f control is implemented to start the motor when the speed reaches above a certain threshold, then it is switched to sensorless control.

Traditionally, SMO are used with signum function but chattering is one of the major issue in SMO implementation. In this project, SMO is implemented with saturation function. Further, SMO is implemented with sigmoid function which simplifies the system.

### 5.2.1. Mathematical Modelling

The mathematical model of PMSM alpha beta frame is given by following equations:

$$L_S \left( \frac{d\hat{i}_\alpha}{dt} \right) = -R_S i_\alpha - e_\alpha + u_\alpha \quad (5.1)$$

$$L_S \left( \frac{d\hat{i}_\beta}{dt} \right) = -R_S i_\beta - e_\beta + u_\beta \quad (5.2)$$

$i_\alpha, i_\beta, e_\alpha, e_\beta, u_\alpha, u_\beta$  are the phase currents, back emf and phase voltages in alpha-beta reference frame.  $L_S$  is the stator inductance and  $R_S$  is the stator resistance.

The back emf equations are given by

$$e_\alpha = -\varphi_f \omega_r \sin \theta \quad (5.3)$$

$$e_\beta = \varphi_f \omega_r \cos \theta \quad (5.4)$$

Where,  $\varphi_f$  is the flux linkage of the permanent magnet ,  $\omega_r$  is the electrical angular velocity,  $\theta$  is the electrical rotor position . It can be noticed that the the back emf of motor contain the information of rotor position and speed, but it cannot be measured directly.

By using the mathematical model of PMSM in (1), the SMO equation is shown as follows

$$L_S \left( \frac{d\hat{i}_\alpha}{dt} \right) = -R_S \hat{i}_\alpha + u_\alpha - k(l\overline{Z_{eq,\alpha}} + \overline{Z_\alpha}) \quad (5.5)$$

$$L_S \left( \frac{d\hat{i}_\beta}{dt} \right) = -R_S \hat{i}_\beta + u_\beta - k(l\overline{Z_{eq\beta}} + \overline{Z_\beta}) \quad (5.6)$$

$$l = \begin{cases} -0.5 & n < 375 \text{ rpm} \\ 1 & n > 750 \text{ rpm} \end{cases}$$

$l$  is the feedback gain of the equivalent control  $\overline{Z_{eq}}$ , and  $k$  is the switching gain of the discontinuous control for the signum function. The value of switching gain must be just above the maximum amplitude of back emf.

$$\overline{Z} = -K * \text{sign}(\hat{i}_s - i_s)$$

The equivalent  $\overline{Z_{eq}}$  is given by,

$$\overline{Z_{eq}} = \frac{1}{1 + p\tau} \overline{Z}$$

$$p = \frac{d}{dt}$$

To reduce the effect of chattering, the signum function is replaced by saturation

### **Saturation function**

If the value of  $\hat{i}_s - i_s$  is less than  $E_0$ , the value of control signal

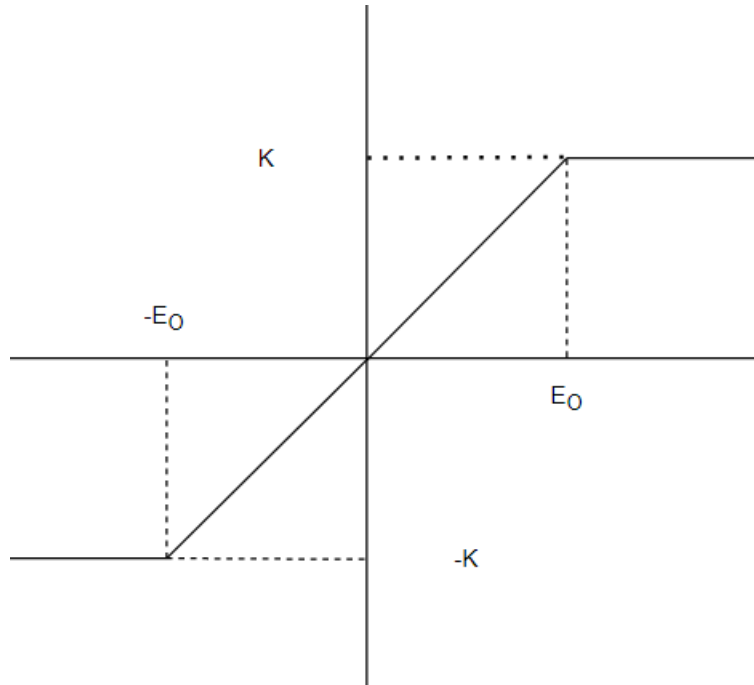
$$\overline{Z} = -K_S (\hat{i}_s - i_s), \text{ where } K_S = \frac{K}{E_0}$$

Else  $\overline{Z} = K$

Then the equation for sliding mode observer are written as,

$$L_S \left( \frac{d\hat{i}_\alpha}{dt} \right) = -R_S \hat{i}_\alpha + u_\alpha - (1 + l)\overline{Z_{eq\alpha}} \quad (5.7)$$

$$L_S \left( \frac{d\hat{i}_\beta}{dt} \right) = -R_S \hat{i}_\beta + u_\beta - (1+l) \overline{Z_{eq\beta}} \quad (5.8)$$



5.2

Saturation Function

## 5.2.2. Stability Analysis

Verifying the stability of the modified SMO, the Lyapunov function is

$$V = \frac{1}{2} \mathbf{S}(\mathbf{X})^T \mathbf{S}(\mathbf{X}) \quad (5.9)$$

Where  $\mathbf{S}(\mathbf{X}) = \begin{bmatrix} \bar{i}_\alpha \\ \bar{i}_\beta \end{bmatrix}$

$$\bar{i}_\alpha = \hat{i}_\alpha - i_\alpha$$

$$\bar{i}_\beta = \hat{i}_\beta - i_\beta$$

The stability condition is defined as following:

$$\dot{V} = \mathbf{S}(\mathbf{X})^T \dot{\mathbf{S}}(\mathbf{X}) \leq \mathbf{0}$$

the error equation is obtained by subtracting (1) from (5) as

$$L_S[\dot{S}_\alpha(X)] = -R_S S_\alpha(X) + e_\alpha - (1+l)k\overline{Z_{eq\alpha}} \quad (5.10)$$

$$L_S[\dot{S}_\beta(X)] = -R_S S_\beta(X) + e_\beta - (1+l)k\overline{Z_{eq\beta}} \quad (5.11)$$

Therefore, we have

$$\dot{V} = [\bar{i}_\alpha \quad \bar{i}_\beta] \begin{bmatrix} -\frac{R_S \bar{i}_\alpha}{L_S} + \frac{e_\alpha}{L_S} - \frac{k}{L_S} (1+l)\overline{Z_{eq\alpha}} \\ -\frac{R_S \bar{i}_\beta}{L_S} + \frac{e_\beta}{L_S} - \frac{k}{L_S} (1+l)\overline{Z_{eq\beta}} \end{bmatrix} \quad (5.12)$$

$$\dot{V} = \left[ -\left( \frac{R_S}{L_S} \bar{i}_\alpha^2 + \frac{R_S}{L_S} \bar{i}_\beta^2 \right) \right] + \left[ \frac{1}{L_S} (e_\alpha - k(1+l)\overline{Z_{eq\alpha}}) \bar{i}_\alpha + \frac{1}{L_S} (e_\beta - k(1+l)\overline{Z_{eq\beta}}) \bar{i}_\beta \right] \quad (5.13)$$

The first term in the equation is less than zero hence, the second term in the above equation must be less than zero. Therefore the observer gain must be

$$k > \max\left(\left|\frac{e_\alpha}{Z_\alpha}\right|, \left|\frac{e_\beta}{Z_\beta}\right|\right) \quad (5.14)$$

If  $k$  is large enough then the SMO is asymptotically stable and converges to its sliding surface

Then

$$\mathbf{S}(\mathbf{X}) = \dot{\mathbf{S}}(\mathbf{X}) = \mathbf{0}$$

From the above equation we have

$$e_\alpha = (1 + l)\overline{Z_\alpha} \quad (5.15)$$

$$e_\beta = (1 + l)\overline{Z_\beta} \quad (5.16)$$

### 5.2.3. Phase compensation module

As observed from the above equation lpf is required for removal of chattering in the system, this introduces delay in the system which has to be appropriately compensated. Hence a phase compensation module is required. Various phase compensation techniques are implemented in the literature. In this project low pass filter is implemented where lpf filter cut-off frequency is function of the rotor velocity.

$$\omega_{cutoff} = k\omega_{elec}$$

$$lpf = \frac{k\omega_{elec}}{j\omega_{elec} + k\omega_{elec}}$$

Phase compensation required  $\tan^{-1} \frac{1}{k}$

Therefore only constant compensation is required in the rotor angle at all the rotor velocity.



### 5.2.4. Rotor velocity estimation

There are two methods available for rotor velocity one is differentiating the rotor angle

$$\omega_{elec} = \frac{d}{dt}\theta \quad (5.17)$$

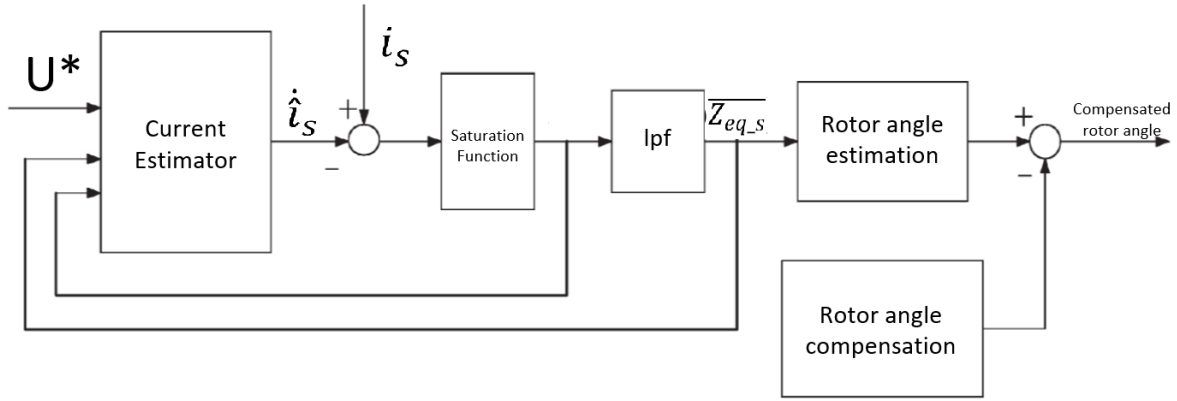
Where  $\theta$  is the rotor angle. This method gives a lot of noise because of presence of chattering present in rotor angle, therefore this method is not preferred in this project. Second method use the back emf model,

$$\omega_{elec} = \frac{\sqrt{e_{\alpha}^2 + e_{\beta}^2}}{\varphi} \quad (5.18)$$

We can observe that the rotor velocity depend upon the flux linkage which varies during operation. Therefore, flux linkage estimation is required for rotor velocity estimation.

### 5.2.5. Simulation

SMO with saturation function is implemented in this project. In this, smo is implemented with gain  $l$  is implemented, which take into account of the low resolution of the back emf at low speed. Figure 5.3 shows the scheme of sliding mode observer modelled in Simulink matlab. Here,  $U^*$  is the stator terminal voltage.



5.3 Simulated Sliding mode observer

$$L_S \left( \frac{d\hat{i}_\alpha}{dt} \right) = -R_S i_\alpha + u_\alpha - (1 + l) \overline{Z_{eq\_a}}$$

$$L_S \left( \frac{d\hat{i}_\beta}{dt} \right) = -R_S i_\beta + u_\beta - (1 + l) \overline{Z_{eq\_b}}$$

Where,

$$l = \begin{cases} -0.5 & n < 375 \text{ rpm} \\ 1 & n > 375 \text{ rpm} \end{cases}$$

$$\overline{Z_{eq\beta}} = \frac{1}{1 + p\tau} \overline{Z_\beta}$$

$$p = \frac{d}{dt}$$

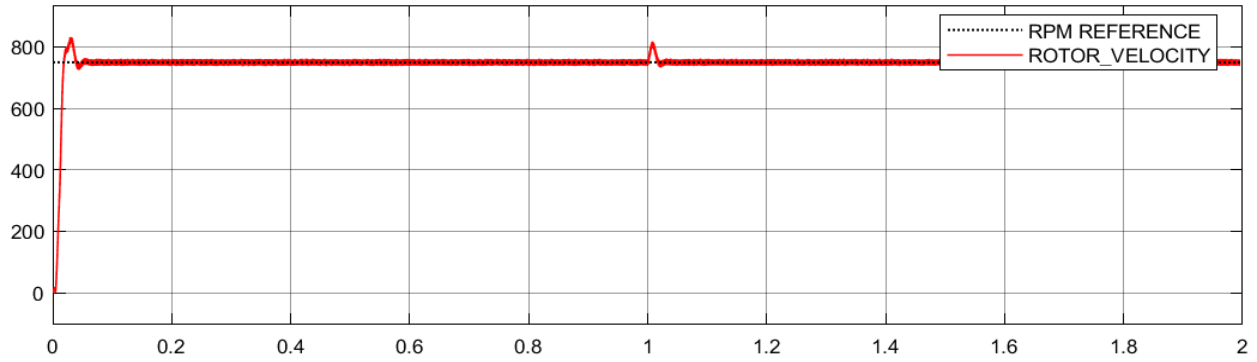
The simulation is conducted with  $l=1$  for all the speed range, so as to further not complicate the model.

In this section speed control of PMSM is implemented in sensorless mode. This is divided into three section.

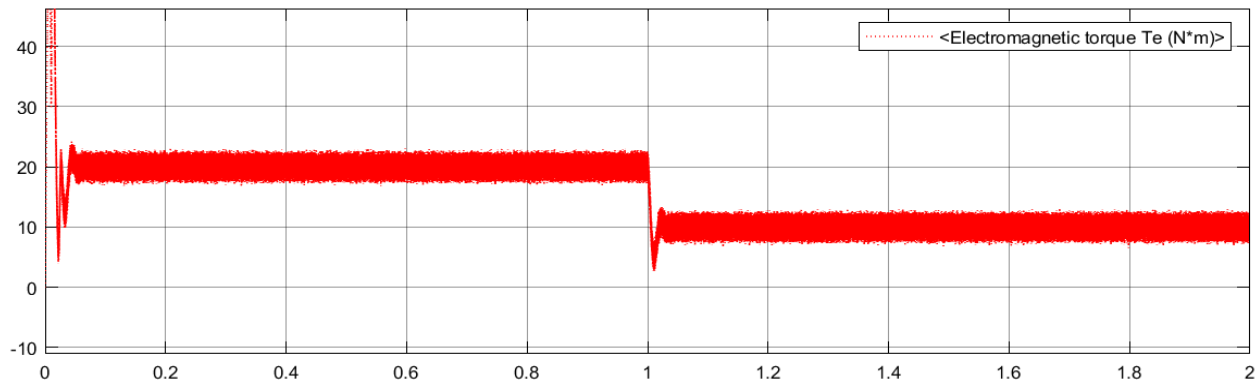
1. The speed reference is changed from 0 to 750 rpm with rated load torque of 20 Nm. Then, the load torque is changed from 20 Nm to 10 Nm at 750 rpm. Rotor angular velocity,  $I_d$  and  $I_q$ , electromagnetic torque developed are analysed
2. Estimated rotor angle, rotor angle are analysed
  - 2.1 Speed reference is changed 400 rpm to 750 rpm at 1 sec with constant torque load of 20 Nm
  - 2.2 The torque load is changed from 20 Nm to 10 Nm with rated speed of 750 rpm.
3. Estimated alpha-beta stator current and back emf are analysed at 750 rpm and 400 rpm

These test cases are satisfactorily test the performance of motor under the various loading conditions. Simulation should mirror the performance of the drive in real world conditions.

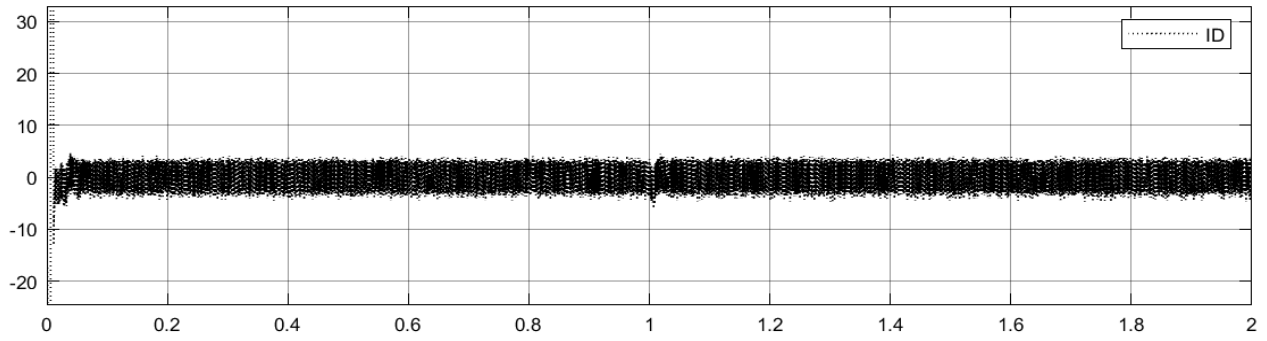
1. The speed reference is changed from 0 to 750 rpm with rated load torque of 20 Nm. Then, the load torque is changed from 20 Nm to 10 Nm at 750 rpm. Rotor angular velocity,  $I_d$  and  $I_q$ , electromagnetic torque developed are analysed



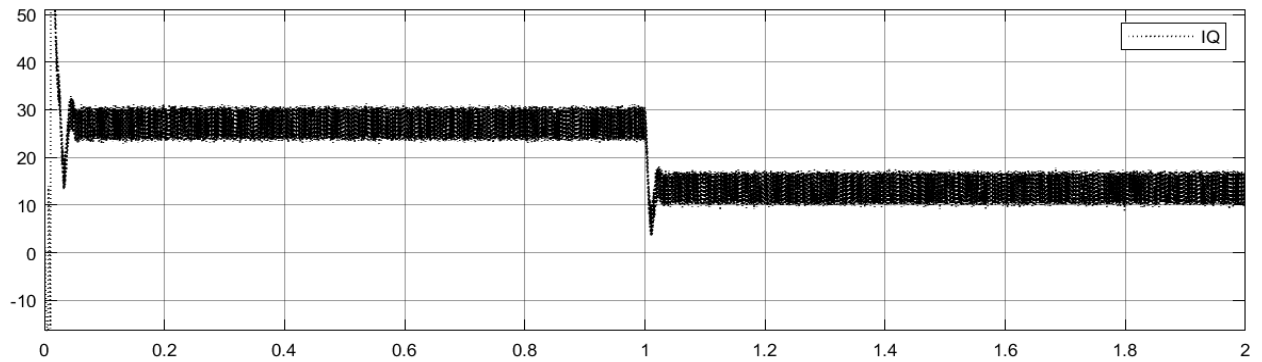
5.4 Rotor velocity



5.5 Electromagnetic Torque



5.6 Id current



5.7 Iq current

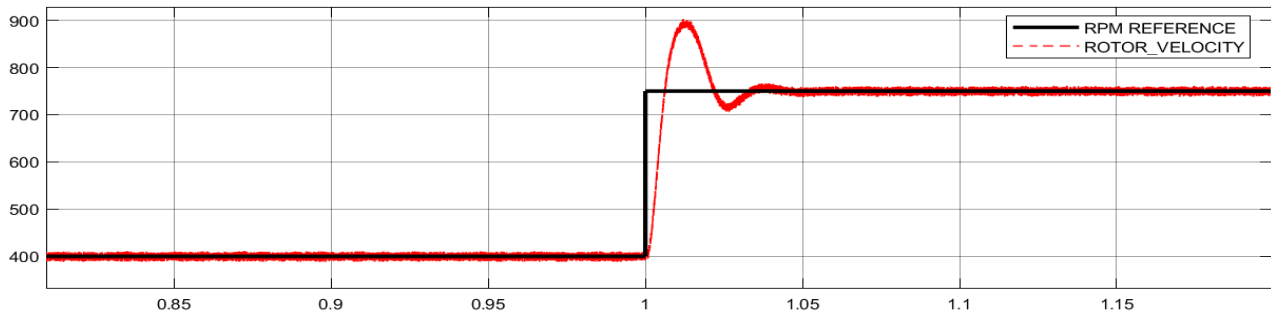
Figure 5.4 , 5.5, 5.6, 5.7 shows the rotor velocity response , electromagnetic torque , Id ad Iq current when the speed reference is changed from 0 to 750 rpm with rated load torque of 20 Nm at 0 s and the load torque is changed from 20 Nm to 10 Nm at 750 rpm at the 1s

2. Estimated rotor angle , rotor angle are analysed

2.1 Speed reference is changed 400 rpm to 750 rpm at 1 sec with constant torque load of 20 Nm

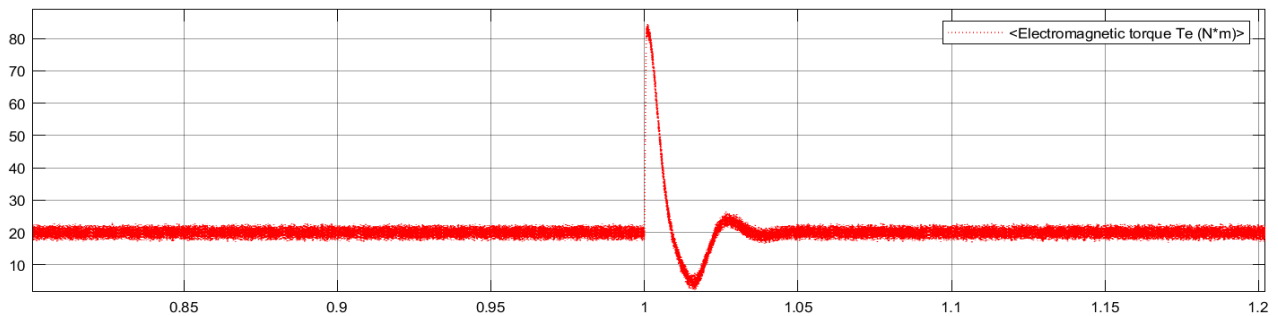
2.2 The torque load is changed from 20 Nm to 10 Nm with rated speed of 750 rpm.

### 2.1 Speed reference is changed 400 rpm to 750 rpm at 1 sec with constant torque load of 20 Nm

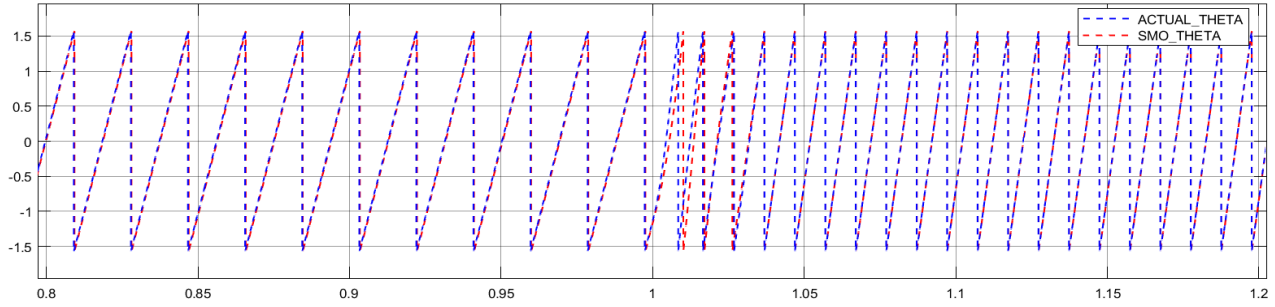


5.8 Rotor Velocity

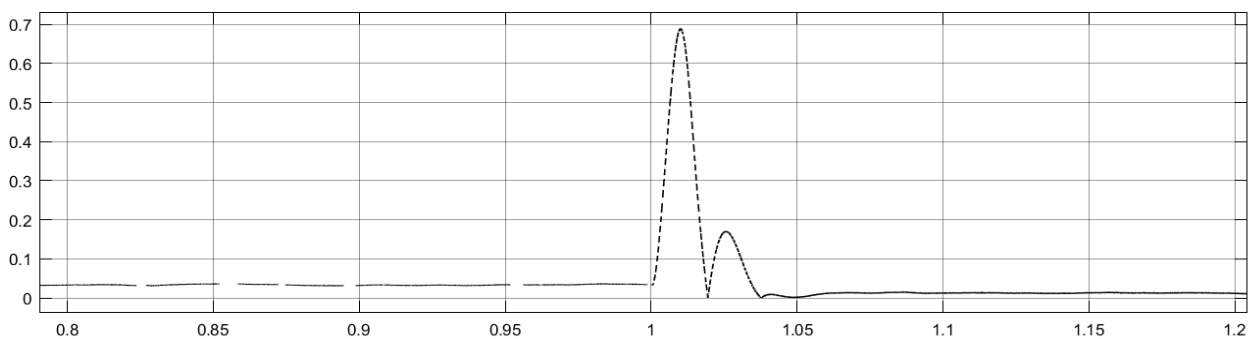
Rotor velocity has certain noise due to inherent nature of sliding mode observer



5.9 Electromagnetic Torque When The Speed Reference Is Changed From 400 Rpm To 750 Rpm At 1 Second



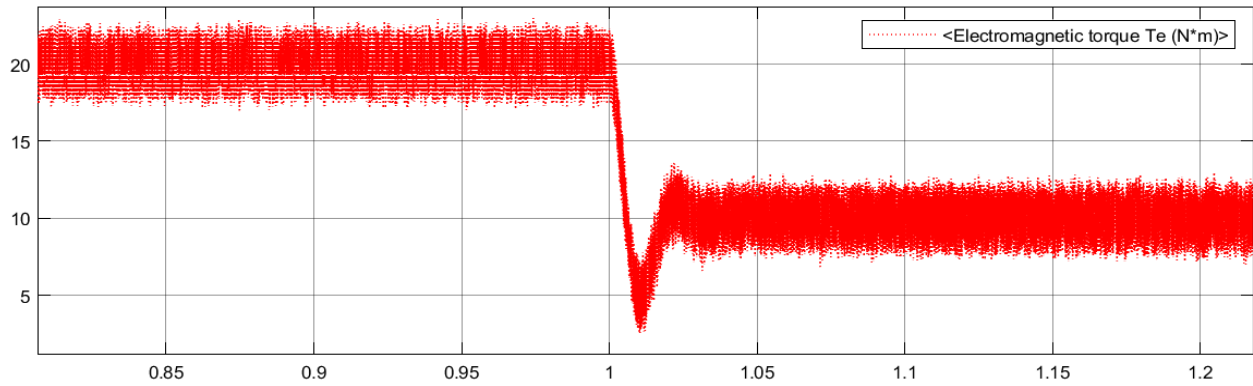
5.10 Electrical Rotor Angle When Speed Reference Is Changed From 400 Rpm To 750 Rpm At 1 Second



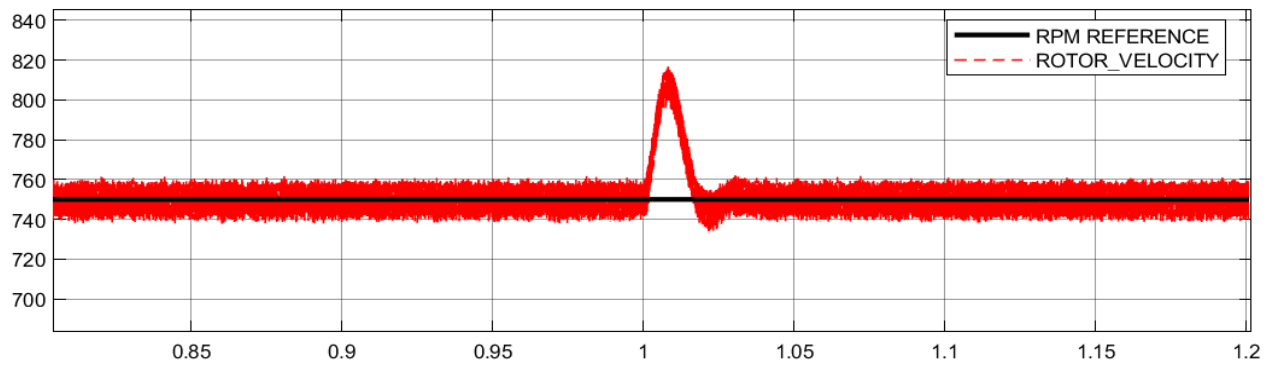
5.11 Electrical Rotor Angle Error B/W The Actual Rotor Angle And Smo Rotor Angle When Speed Reference Is Changed From 400 Rpm To 750 Rpm At 1 Second.

The rotor velocity response with SMO is shown figure 5.8. The developed electromagnetic torque is shown figure 5.9. The estimated rotor angle and the actual rotor angle are compared in figure 5.10 The rotor angle between the actual rotor angle and estimated SMO rotor angle is compared and error b/w them is displayed in figure 5.11 and it is observed that there is significant deviation in estimated rotor angle deviation when the motor is in transient state. It is inferred that this is due to the presence of lpf which provide the phase lag in the system.

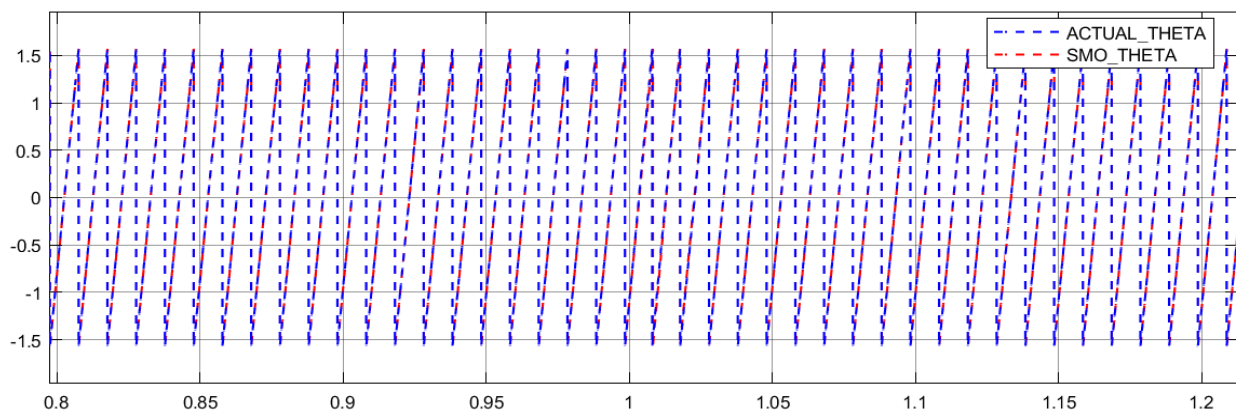
## 2.2 The torque load is changed from 20 Nm to 10 Nm with rated speed of 750 rpm.



### 5.12 Electromagnetic Torque When The Load Torque Is Changed From 20 Nm To 10 Nm At 1 Second Rotor Angle Of The PMSM Motor

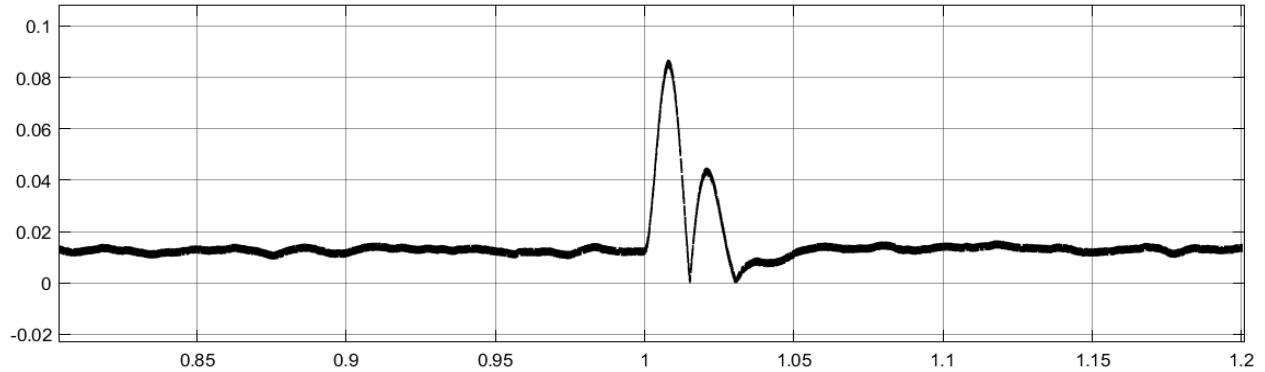


### 5.13 Estimated Rotor Velocity





### 5.11 Rotor angle of the PMSM motor

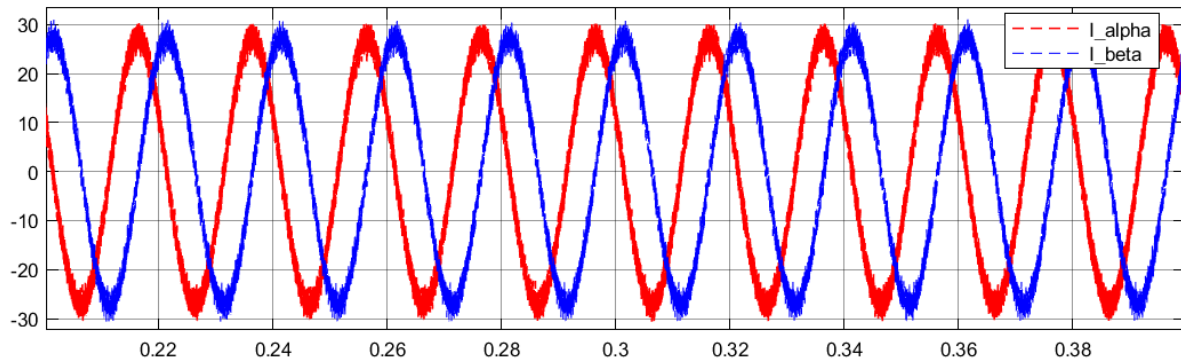


### 5.13 Rotor Angle Error

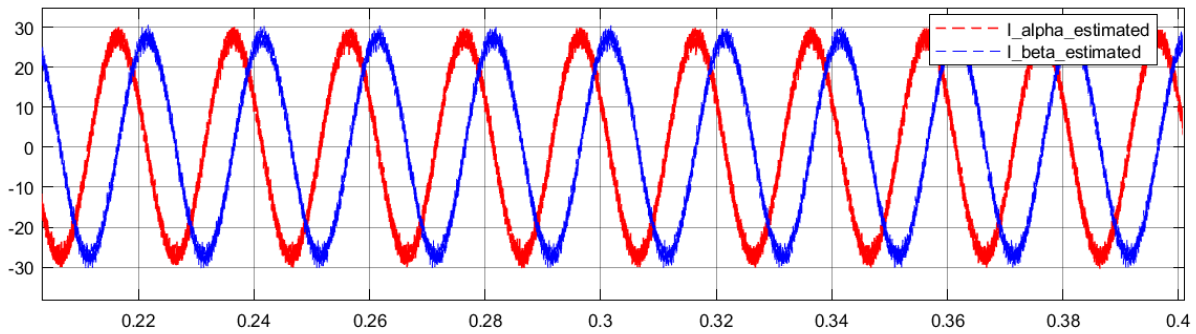
The rotor angle between the actual rotor angle and estimated SMO rotor angle is compared and error b/w them is displayed figure 5.12 and 5.13 , it is observed that there is no significant deviation in estimated rotor angle from true rotor angle deviation when the motor is in transient state.

**Estimated alpha-beta stator current and back emf are analysed at 750 rpm and 400 rpm**

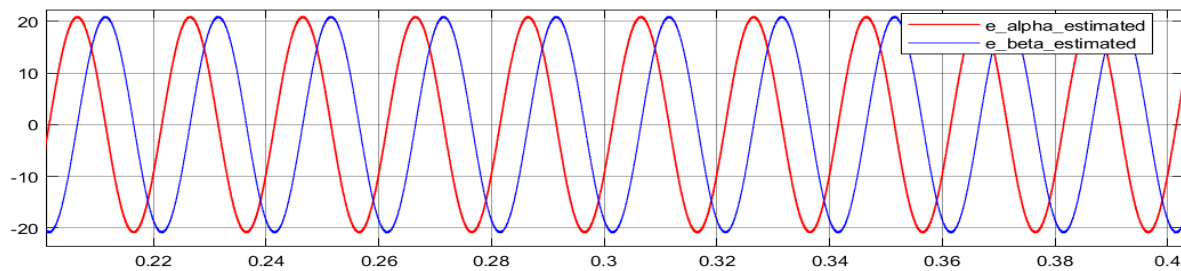
1. at 750 rpm



5.14  $i_{\alpha}, i_{\beta}$  Of The PMSM At 750 Rpm I.E. Current In The Stator At 50 Hz

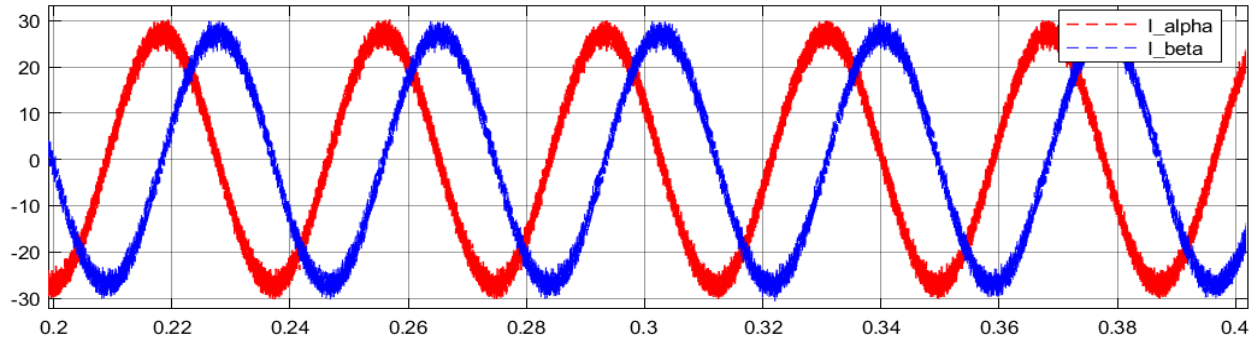


5.15  $\hat{i}_{\alpha}, \hat{i}_{\beta}$  Of The PMSM At 750 Rpm I.E. Current In The Stator At 50 Hz

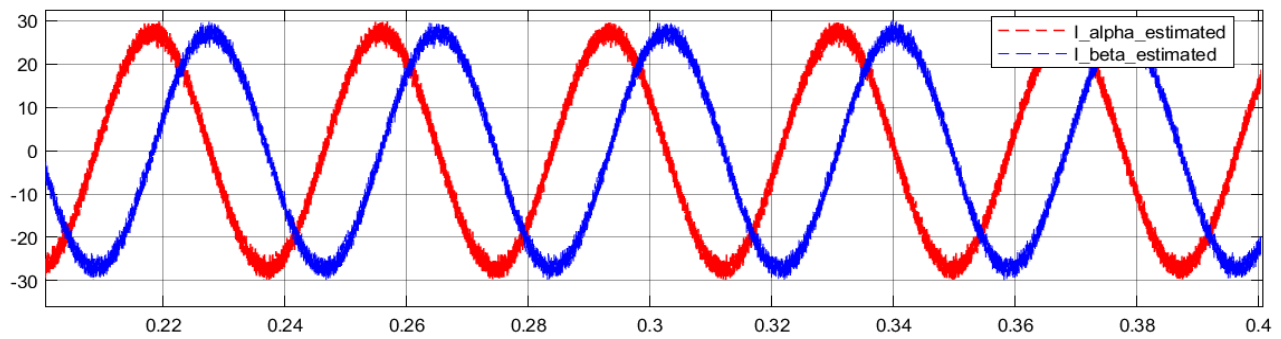


5.16  $\hat{e}_{\alpha}, \hat{e}_{\beta}$  Of The PMSM At 750 Rpm I.E. Current In The Stator At 50 Hz

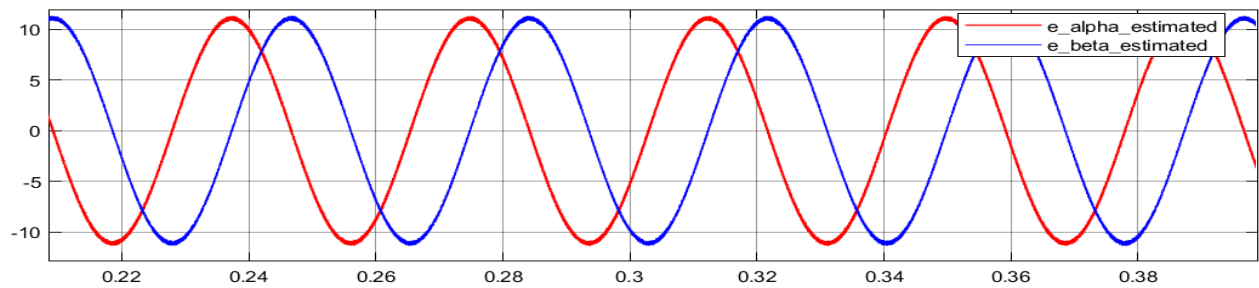
2. at 400 rpm



5.17  $i_\alpha, i_\beta$  Of The PMSM At 400 Rpm I.E. Current In The Stator At 26.66 Hz



5.18  $\hat{i}_\alpha, \hat{i}_\beta$  Of The PMSM At 400 Rpm I.E. Current In The Stator At 26.66 Hz



5.19  $\hat{e}_\alpha, \hat{e}_\beta$  Of The PMSM At 400 Rpm I.E. Current In The Stator At 26.66 Hz

The figures 5.18 and 5.15 show the good current tracking performance of the proposed smc at 400 and 750 rpm. The back emf are satisfactorily estimated at both the speed for the estimated of rotor position and speed. As observed, Chattering is reduced considerably in the estimated back emf due to lpf shown in figure 5.16 ad 5.19 .

### 5.3. Modified SMO

In order to reduce chattering instead of saturation function, continuous sigmoid function is proposed

$$F(x) = \frac{1}{e^{n\bar{t}_x} + 1} \quad (5.19)$$

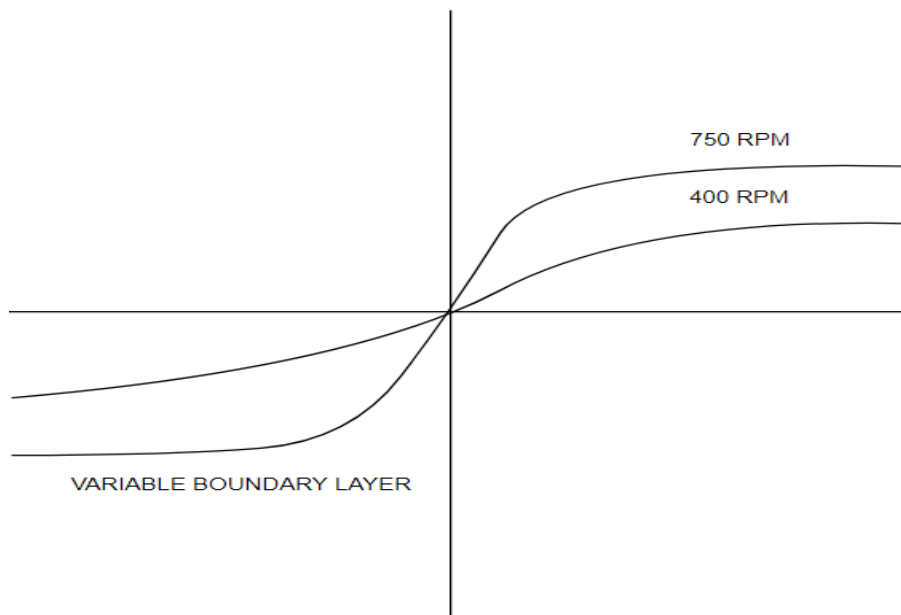
Where n is a positive constant. The function is similar to saturation function with non-linear slope and has no time delay characteristics.

#### 5.3.1 Sigmoid as a switching function

This section proposes a new sensorless control algorithm for a PMSM based on the new SMO which uses a sigmoid function as a switching function with variable boundary layers[].

$$\text{boundary layer} = k\omega_{elec} \quad (5.20)$$

SMO with lpf introduces delay in the system, due to which there is a significant deviation in estimated rotor angle in transient state. So, a new SMO is defined with sigmoid function having variable boundary layer, without lpf is introduced. The boundary layer of the sigmoid is proportional to the electrical rotor velocity of the motor.



5.20 Sigmoid function with variable boundary layer

### 5.3.2. Mathematical Modelling

Then the smo can be written as ,

$$L_S \left( \frac{d\hat{i}_\alpha}{dt} \right) = -R_S i_\alpha + u_\alpha - kF(\bar{i}_\alpha) \quad (5.21)$$

$$L_S \left( \frac{d\hat{i}_\beta}{dt} \right) = -R_S i_\beta + u_\beta - kF(\bar{i}_\beta) \quad (5.22)$$

Where, F(i) is the sigmoid switching function

### 5.3.3. Stability Analysis

Verifying the stability of the modified SMO, the Lyapunov function is

$$V = \frac{1}{2} \mathbf{S}(\mathbf{X})^T \mathbf{S}(\mathbf{X}) \quad (5.23)$$

Where  $\mathbf{S}(\mathbf{X}) = \begin{bmatrix} \bar{i}_\alpha \\ \bar{i}_\beta \end{bmatrix}$

The stability condition is defined as following:

$$\dot{V} = \mathbf{S}(\mathbf{X})^T \dot{\mathbf{S}}(\mathbf{X}) \leq \mathbf{0}$$

the error equation is obtained by subtracting (1) from (5) as

$$L_S [\dot{S}_\alpha(X)] = -R_S S_\alpha(X) + e_\alpha - kF(\bar{i}_\alpha) \quad (5.24)$$

$$L_S [\dot{S}_\beta(X)] = -R_S S_\beta(X) + e_\beta - kF(\bar{i}_\beta) \quad (5.25)$$

Therefore, we have

$$\dot{V} = [\bar{i}_\alpha \quad \bar{i}_\beta] \begin{bmatrix} -\frac{R_S \bar{i}_\alpha}{L_S} + \frac{e_\alpha}{L_S} - \frac{k}{L_S} F(\bar{i}_\alpha) \\ -\frac{R_S \bar{i}_\beta}{L_S} + \frac{e_\beta}{L_S} - \frac{k}{L_S} F(\bar{i}_\beta) \end{bmatrix} \quad (5.26)$$

$$\dot{V} = \left[ -\left( \frac{R_S}{L_S} \bar{i}_\alpha^2 + \frac{R_S}{L_S} \bar{i}_\beta^2 \right) \right] + \left[ \frac{1}{L_S} (e_\alpha - kF(\bar{i}_\alpha)) \bar{i}_\alpha + \frac{1}{L_S} (e_\beta - kF(\bar{i}_\beta)) \bar{i}_\beta \right] \quad (5.27)$$

The first term in the equation is less than zero hence, the second term in the above equation must be less than zero. Therefore the observer gain must be

$$k > \max \left( \left| \frac{e_\alpha}{F(\bar{l}_\alpha)} \right|, \left| \frac{e_\beta}{F(\bar{l}_\beta)} \right| \right) \quad (5.28)$$

If  $k$  is large enough then the smo is asymptotically stable and converges to its sliding surface

Then

$$\mathbf{S}(\mathbf{X}) = \dot{\mathbf{S}}(\mathbf{X}) = \mathbf{0}$$

From the above equation we have

$$e_\alpha = kF(\bar{l}_\alpha) \quad (5.29)$$

$$e_\beta = kF(\bar{l}_\beta) \quad (5.30)$$

### 5.3.4. Estimation of Rotor position and speed

For high performance applications,  $e_\alpha$  and  $e_\beta$  cannot be used for rotor position determination as the signal still contains high-frequency components. Traditionally, a first-order low-pass filter is commonly used in smo for filtering, thus causing phase delay. Therefore phase compensation is required, since the real-time rotor velocity information is required, the dynamic performance is affected. Therefore, in order to avoid the use of the low-pass filter and phase compensation part, based on the back EMF model from [30], This paper constructs an observer to obtain the back EMF signal so as to estimate rotor position and speed.

Because the change rate of motor angular velocity is far less than that of stator current, assuming  $\dot{\omega}_r = 0$ , then the back EMF model of PMSM can be expressed as

$$\frac{de_\alpha}{dt} = -\omega_r e_\beta \quad (5.31)$$

$$\frac{de_\beta}{dt} = \omega_r e_\alpha$$

Based on the above equations, a back EMF observer is constructed

$$\frac{d\widehat{e}_\alpha}{dt} = -\widehat{\omega}_r \widehat{e}_\beta - l(\widehat{e}_\alpha - e_\alpha) \quad (5.32)$$

$$\frac{d\widehat{e}_\beta}{dt} = \widehat{\omega}_r \widehat{e}_\alpha - l(\widehat{e}_\beta - e_\beta) \quad (5.33)$$

$$\frac{d\widehat{\omega}_r}{dt} = (\widehat{e}_\alpha - e_\alpha)\widehat{e}_\beta - (\widehat{e}_\beta - e_\beta)\widehat{e}_\alpha \quad (5.34)$$

Where,  $l$  is the observer gain. By subtracting (12) from (13) and doing further consolidation, the error equation is obtained as

$$\frac{d\widetilde{e}_\alpha}{dt} = -\widetilde{\omega}_r \widehat{e}_\beta - \omega_r \widehat{e}_\beta - l\widetilde{e}_\alpha \quad (5.35)$$

$$\frac{d\widetilde{e}_\beta}{dt} = \widetilde{\omega}_r \widehat{e}_\alpha + \omega_r \widehat{e}_\alpha - l\widetilde{e}_\beta \quad (5.36)$$

$$\frac{d\widetilde{\omega}_r}{dt} = \widetilde{e}_\alpha \widehat{e}_\beta - \widehat{e}_\beta \widetilde{e}_\alpha \quad (5.37)$$

Where  $\widetilde{e}_\alpha = \widehat{e}_\alpha - e_\alpha$ ,  $\widetilde{e}_\beta = \widehat{e}_\beta - e_\beta$  and  $\widetilde{\omega}_r = \widehat{\omega}_r - \omega_r$ .

Back emf observer gain  $l$ , does not significantly affect the back emf estimation but affects the speed convergence. Lower the  $l$ , higher the speed convergence.

To prove the stability of (5.32), the Lyapunov function is defined as

$$V = \frac{\widetilde{e}_\alpha^2 + \widetilde{e}_\beta^2 + \widetilde{\omega}_r^2}{2} \quad (5.38)$$

Differentiating the above equation

$$\dot{V} = \widetilde{e}_\alpha \dot{\widetilde{e}}_\alpha + \widetilde{e}_\beta \dot{\widetilde{e}}_\beta + \widetilde{\omega}_r \dot{\widetilde{\omega}}_r \quad (5.39)$$

Substituting (14) into the above equation yields

$$\dot{V} = -l(\widetilde{e}_\alpha^2 + \widetilde{e}_\beta^2) \quad (5.40)$$

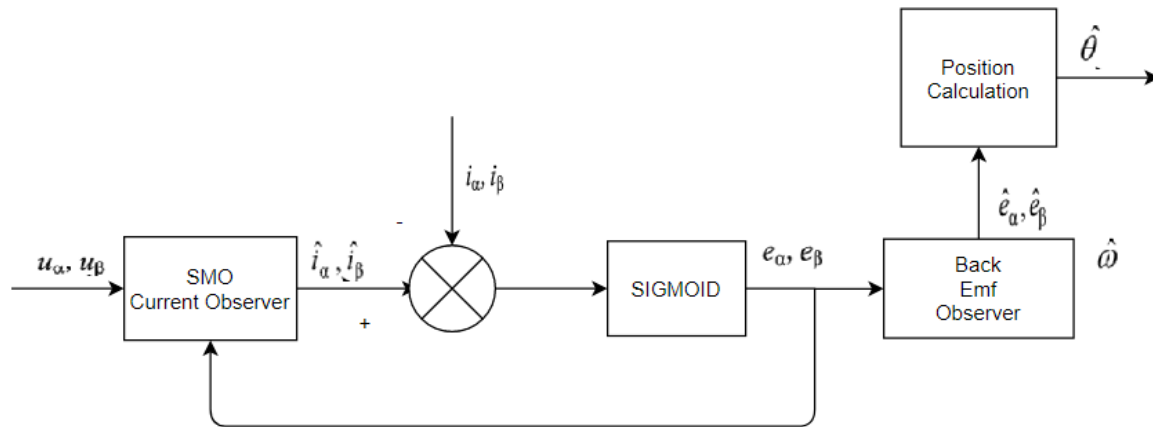
If  $l > 0$ , then the back EMF observer is asymptotically stable and  $\widehat{e}_\alpha, \widehat{e}_\beta$  tend to  $e_\alpha, e_\beta$ . Therefore, by using the back EMF signal obtained from the observer and the relationship between the back EMF and the rotor position, the position signal is estimated as

$$\hat{\theta} = -\arctan\left(\frac{e_\alpha}{e_\beta}\right) \quad (5.41)$$

The rotor speed can be easily obtained from by integral operation of observer. Although the integral operation of observer induces a certain delay in angle estimation which should be appropriately compensated.

The figure 5.21 shows the control diagram of proposed SMO,  $u_\alpha, u_\beta$  are the voltage across motor terminals is used to somehow, mitigate the dead time effect of inverter, Thus rotor position and speed estimation is improved.





## 5.21 Simulated Sliding Mode Observer

### 5.3.5. Simulation

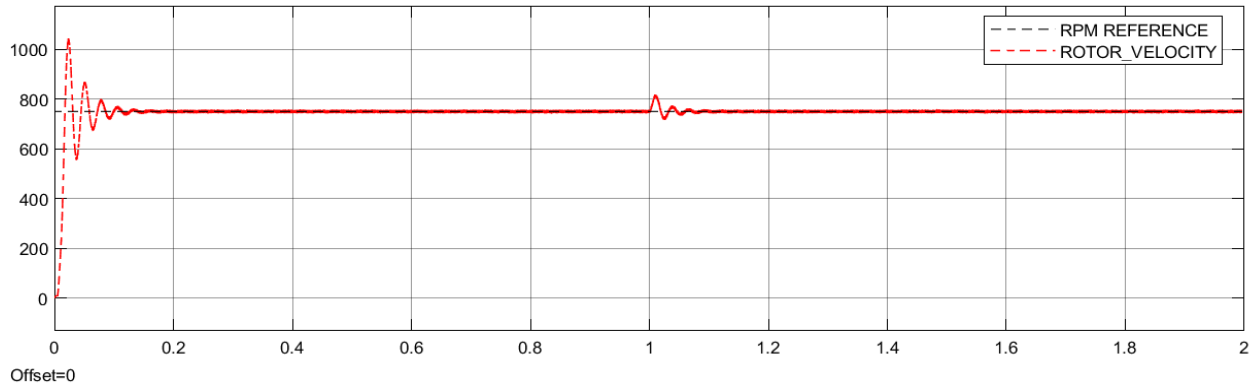
In this section speed control of PMSM is implemented in sensorless mode.

This is divided into three section.

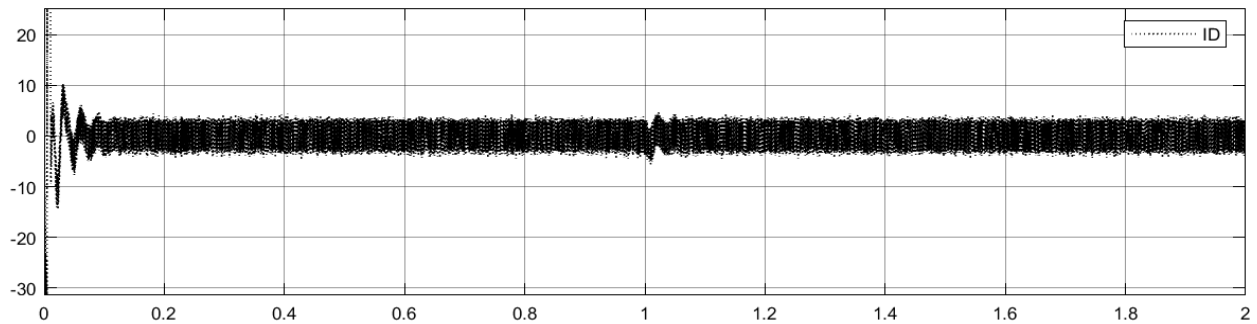
1. The speed reference is changed from 0 to 750 rpm with rated load torque of 20 Nm. Then, the load torque is changed from 20 Nm to 10 Nm at 750 rpm. Rotor angular velocity,  $I_d$  and  $I_q$ , electromagnetic torque developed are analysed
2. Estimated rotor angle, rotor angle are analysed
  - 2.1 Speed reference is changed 400 rpm to 750 rpm at 1 sec with constant torque load of 20 Nm
  - 2.2 The torque load is changed from 20 Nm to 10 Nm with rated speed of 750 rpm.
3. Estimated alpha-beta stator current and back emf are analysed at 750 rpm and 400 rpm

These test cases are satisfactorily test the performance of motor under the various loading conditions. Simulation should mirror the performance of the drive in real world conditions.

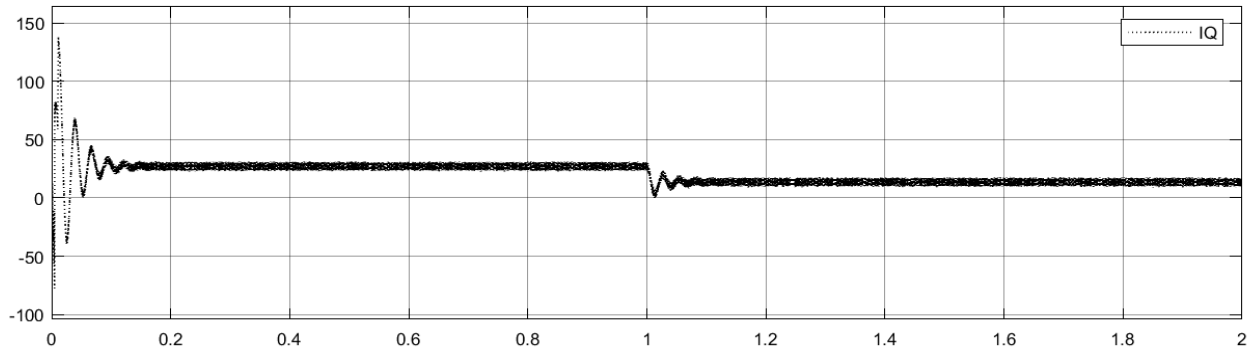
1. The speed reference is changed from 0 to 750 rpm with rated load torque of 20 Nm. Then, the load torque is changed from 20 Nm to 10 Nm at 750 rpm. Rotor angular velocity,  $I_d$  and  $I_q$ , electromagnetic torque developed are analysed



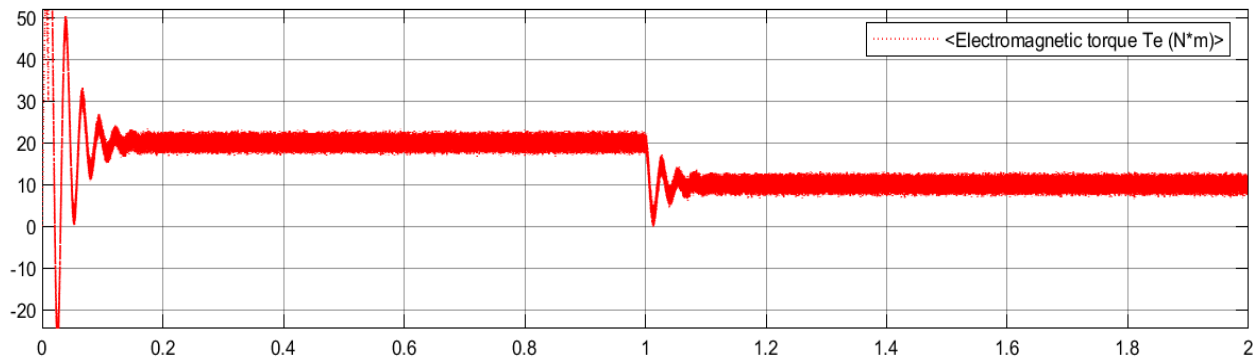
5.22 Rotor velocity



5.23 Id Current



5.24  $I_q$  Current



5.25 Electromagnetic Torque

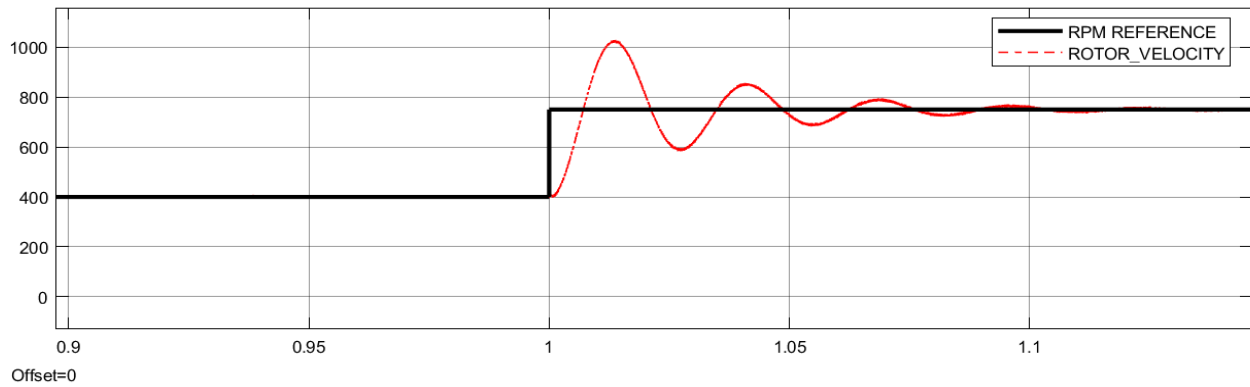
Figure 5.22 , 5.23, 5.24, 5.25 shows the rotor velocity response ,  $I_d$  ,  $I_q$  current and electromagnetic torque when the speed reference is changed from 0 to 750 rpm with rated load torque of 20 Nm at 0 s and the load torque is changed from 20 Nm to 10 Nm at 750 rpm at the 1 s.

1. Estimated rotor angle and actual rotor angle are analysed

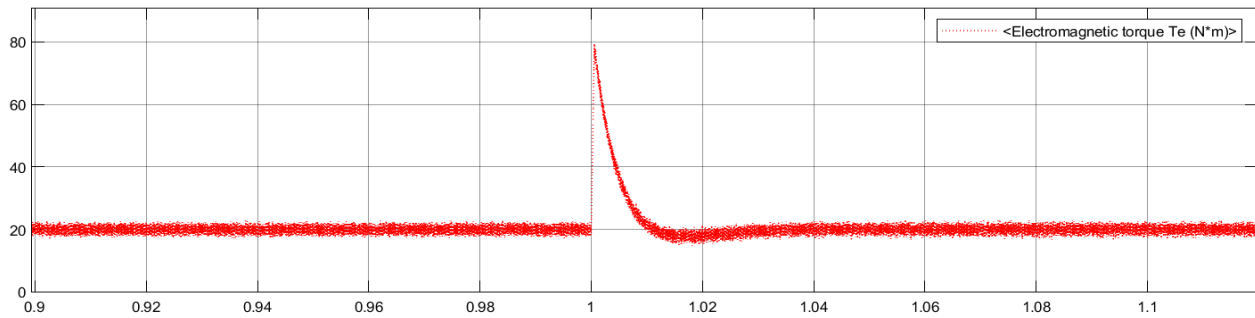
1.1 Speed reference is changed 400 rpm to 750 rpm at 1 sec with constant torque load of 20 Nm

1.2 The torque load is changed from 20 Nm to 10 Nm with rated speed of 750 rpm.

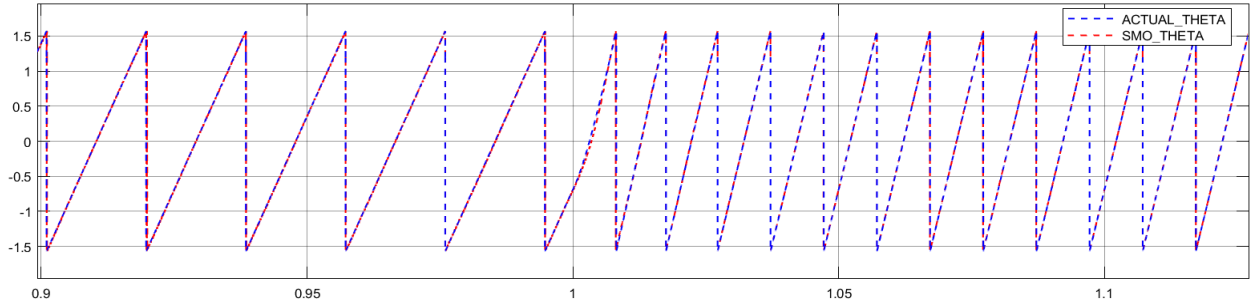
**Speed reference is changed 400 rpm to 750 rpm at 1 sec with constant torque load of 20 Nm**



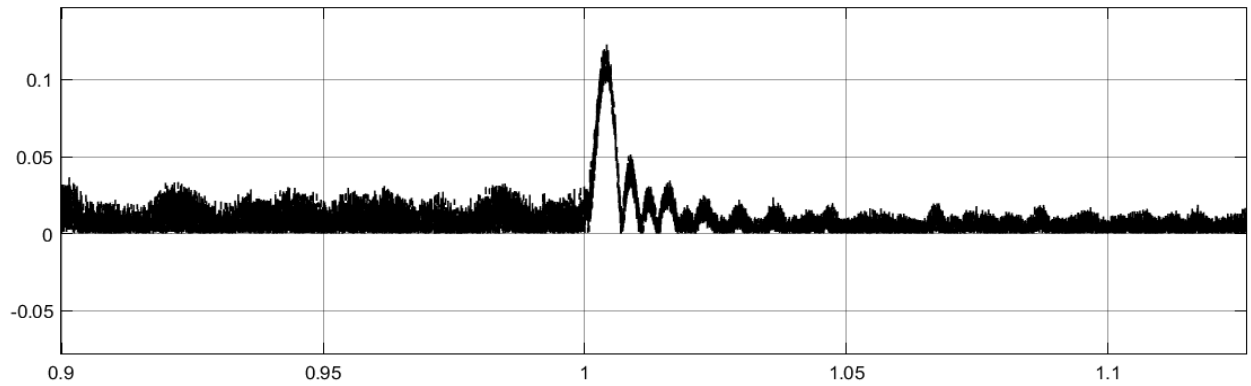
5.26 Rotor Velocity



5.27 Electromagnetic Torque ( $T_e$ )



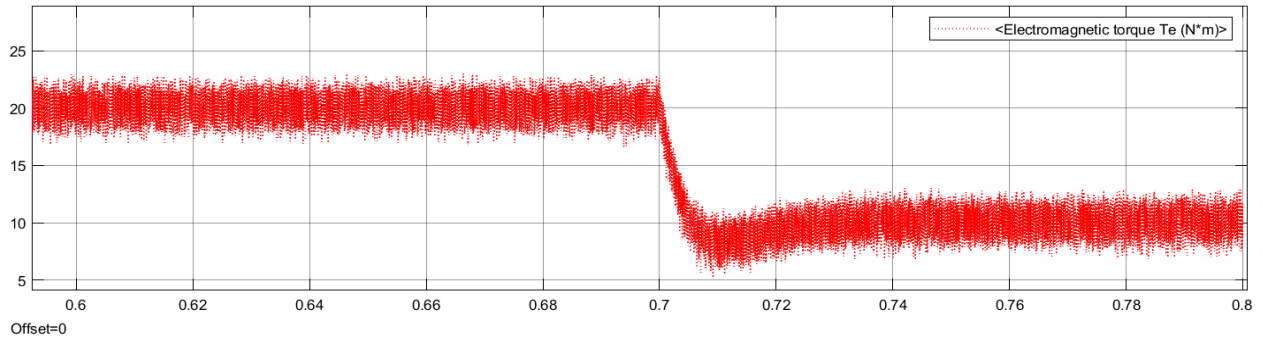
5.28 Rotor Angle



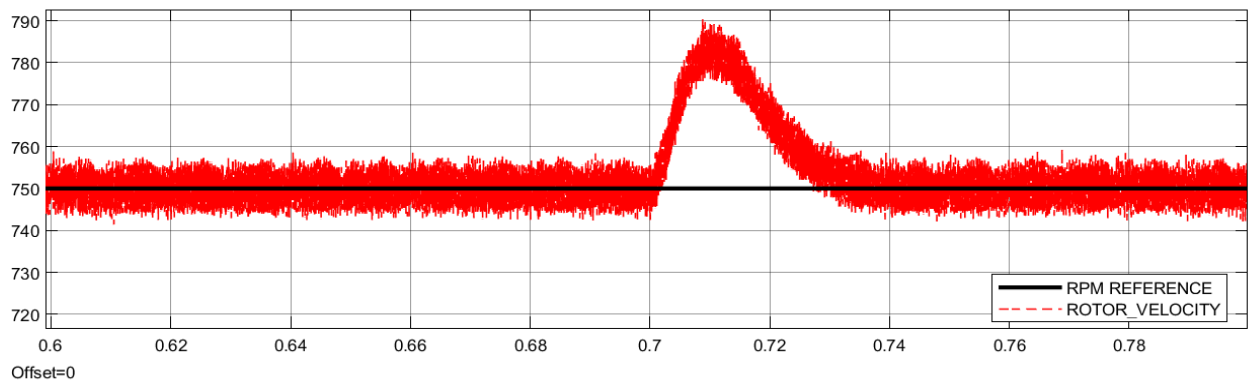
5.29 Estimated Rotor Angle Error

The rotor velocity response with SMO is shown figure 5.26. The Oscillations in estimated rotor in transient state are increased considerably in transient state. The developed electromagnetic torque is shown figure 5.27. The estimated rotor angle and the actual rotor angle are compared in figure 5.28. The rotor angle between the actual rotor angle and estimated SMO rotor angle is compared and error b/w them is displayed in figure 5.29. It is observed that the deviation in estimated rotor angle deviation when the motor is in transient state has reduced considerably in comparison to figure 5.11. It can be inferred that rotor angle estimation is improved widely.

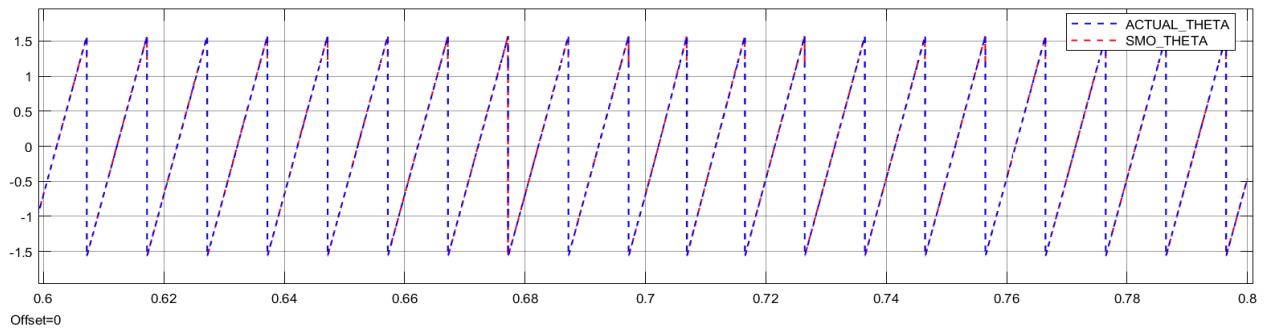
## 2.2 The torque load is changed from 20 Nm to 10 Nm with rated speed of 750 rpm.



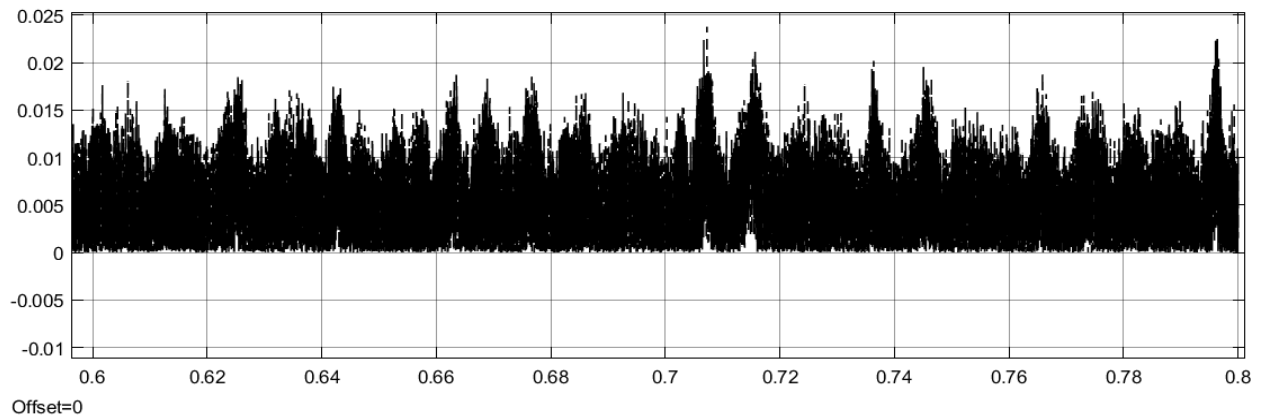
5.30 Electromagnetic Torque



5.31 Rotor Velocity



5.32 Rotor Angle



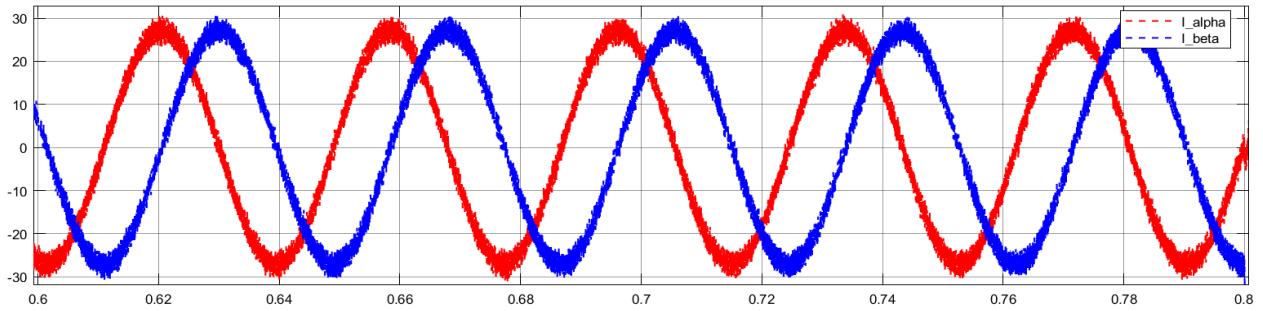
### 5.33 Estimated Rotor Angle Error

The rotor angle between the actual rotor angle and estimated SMO rotor angle is compared and error b/w them is displayed figure 5.32 and 5.33 , it is observed that there is no significant deviation in estimated rotor angle from true rotor angle deviation when the motor is in transient state.

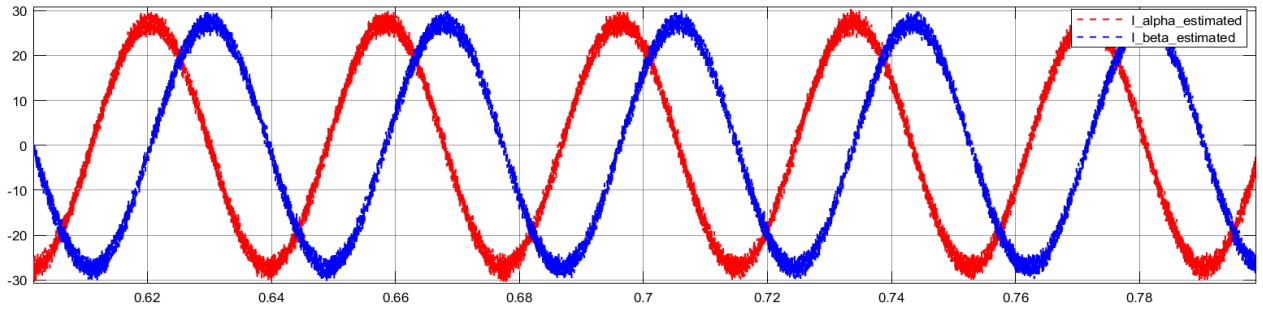
It can be inferred that the accuracy of estimated rotor angle is improved significantly with the proposed new SMO. Hence, rotor angle error is reduced due to the absence of lpf in the new SMO.

3. Estimated alpha-beta stator current and back emf are analysed at 750 rpm and 400 rpm

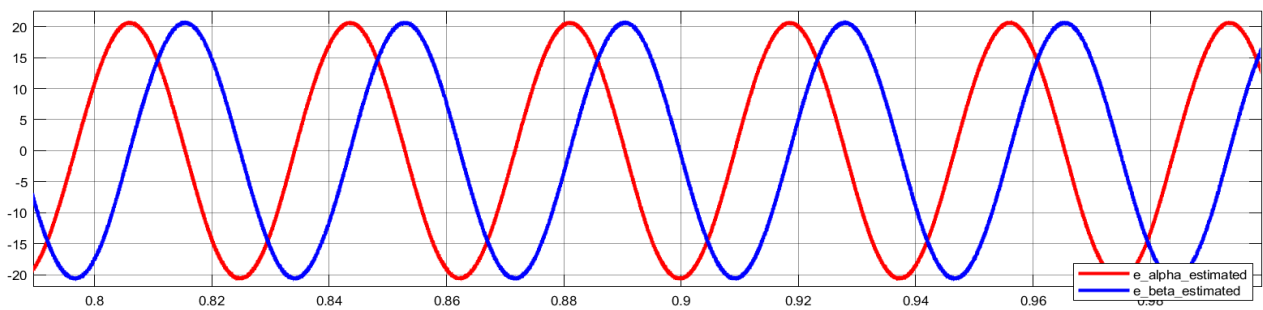
1. at 750 rpm



5.34  $i_{\alpha}, i_{\beta}$  Of The PMSM At 750 Rpm I.E. Current In The Stator At 50 Hz



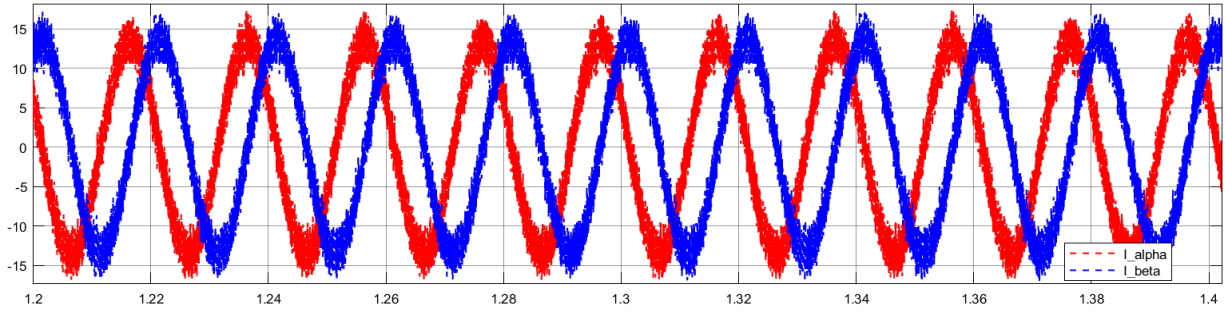
5.35  $\hat{i}_{\alpha}, \hat{i}_{\beta}$  Of The PMSM At 750 Rpm I.E. Current In The Stator At 50 Hz



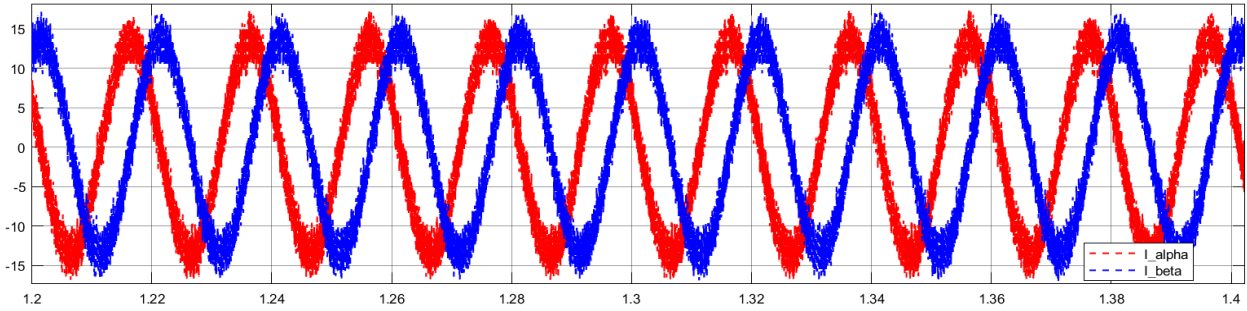
5.36  $\hat{e}_{\alpha}, \hat{e}_{\beta}$  Of The PMSM At 750 Rpm I.E. Current In The Stator At 50 Hz



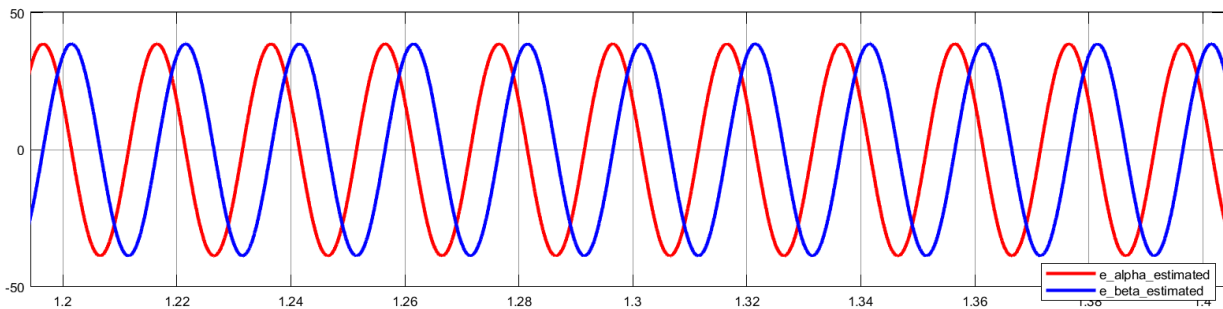
2. at 400 rpm



5.37  $i_{\alpha}, i_{\beta}$  Of The PMSM At 400 Rpm I.E. Current In The Stator At 26.66 Hz



5.38  $\hat{i}_{\alpha}, \hat{i}_{\beta}$  Of The PMSM At 400 Rpm I.E. Current In The Stator At 26.66 Hz



5.39  $\hat{e}_{\alpha}, \hat{e}_{\beta}$  Of The PMSM At 400 Rpm I.E. Current In The Stator At 26.66 Hz

The figures 5.35 and 5.38 show the good current tracking performance of the proposed SMO at 400 and 750 rpm. The back emf are satisfactorily estimated at both the speed as shown in figure 5.36 and 5.39 for the estimated of rotor position and speed.

## 6.5. Discussion

The modified SMO is promising as far as the estimated rotor angle deviation error under dynamic condition is concerned. The rotor angle error is decreased from 0.69 to 0.10 as in figure 5.11 and 5.29 with modified SMO.

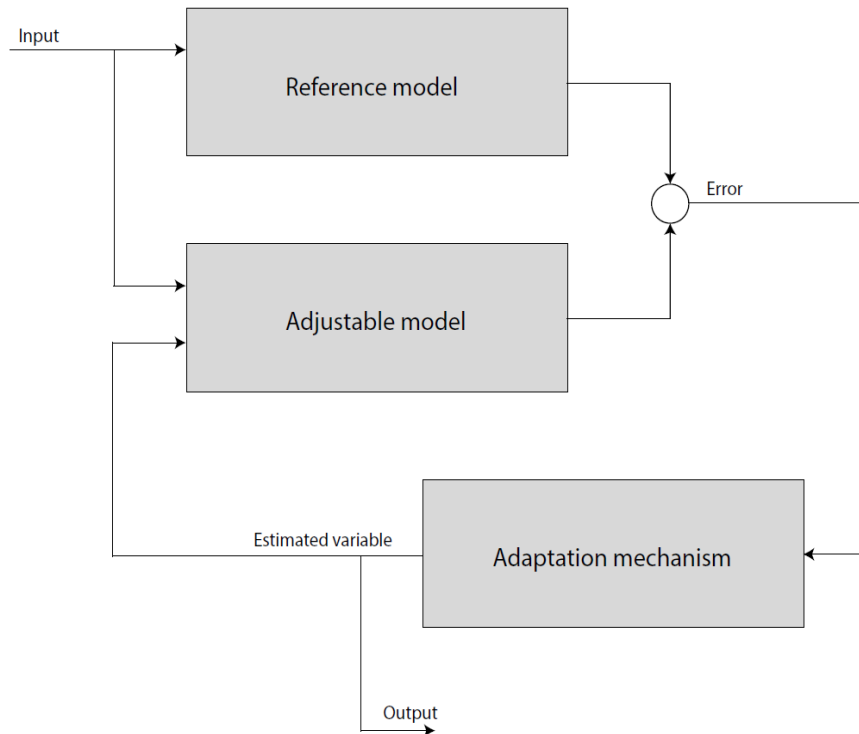
Oscillation are observed in rotor angular velocity in transient state, in the modified SMO as in figure 5.26 in comparison to figure 5.8 This may be attributed to chattering present in the back emf amplitude .Both the SMO promise good stator current tracking performance and back estimation as in 5.15,5.18,5.16 and 5.21 .

As Oscillation are observed in estimated rotor angular velocity in transient state This provided motivation to work on another angular velocity estimation method which estimate the rotor angle by integrating rotor angular velocity.

## Chapter 6

### Model Reference Adaptive System (MRAS)

#### 6.1. Model Reference Adaptive System (MRAS)



#### 6.1 Scheme of Model reference adaptive System

In this project, MRAS is used to estimate the real time rotor velocity which in turn is used to estimate the rotor angle. Two models are used, one is the reference model which is the motor itself and other is the adjustable model which has all the input of the reference model as well has rotor electrical velocity as input. The output current from both the model is compared and fed to the adaptive mechanism. The adaptive mechanism may be the simple PI control, ANN control and SMC. The adaptive mechanism estimate the rotor velocity. The estimated rotor velocity is fed to the adjustable model.

## 6.2. Mathematical Modelling

The state space model of PMSM in dq coordinates is given by:

$$\dot{x} = Ax + Bu \quad (6.1)$$

$$y = Cx \quad (6.2)$$

$$\text{Where } A = \begin{bmatrix} \frac{-R_S}{L_S} & \omega_{el} \\ -\omega_{el} & \frac{-R_S}{L_S} \end{bmatrix}, B = \begin{bmatrix} \frac{v_d}{L_S} \\ \frac{(v_q - \varphi_r \omega_{el})}{L_S} \end{bmatrix}, C = \begin{bmatrix} 1 & 0 \\ 0 & 1 \end{bmatrix}, x = [i_d \ i_q]^T$$

Where  $v_d, v_q, i_d, i_q$  are the rotor voltage and current in dq frame.  $\omega_{el}$  is the rotor velocity.

$R_S, L_S$  are the stator resistance and inductance.

The adjustable model will be the PMSM electrical equations estimated values for the currents and the rotor electrical speed is given by

$$\dot{\hat{x}} = \hat{A}\hat{x} + \hat{B}u \quad (6.3)$$

$$y = C\hat{x} \quad (6.4)$$

Where,

$$\hat{A} = \begin{bmatrix} \frac{-R_S}{L_S} & \widehat{\omega}_{el} \\ -\widehat{\omega}_{el} & \frac{-R_S}{L_S} \end{bmatrix}, \hat{B} = \begin{bmatrix} \frac{v_d}{L_S} \\ \frac{(v_q - \varphi_r \widehat{\omega}_{el})}{L_S} \end{bmatrix},$$

$$\hat{x} = [\widehat{i}_d \ \widehat{i}_q]^T$$

The rotor angle is estimated by integral action

$$\widehat{\theta}_{el} = \int \widehat{\omega}_{el} dt \quad (6.5)$$

the generalized error can be measured  $\epsilon = \hat{x} - x$ . By analyzing the generalized error, the transfer function of the adaptive PI-mechanism can be derived as

$$\widehat{\omega}_{el} = \left( K_p + \frac{K_i}{s} \right) \left[ (\widehat{i}_q - i_q) \left( i_d + \frac{\varphi_r}{L_S} \right) - (\widehat{i}_d - i_d) i_q \right] + \widehat{\omega}_{el}(0) \quad (6.6)$$

### 6.3. Simulation

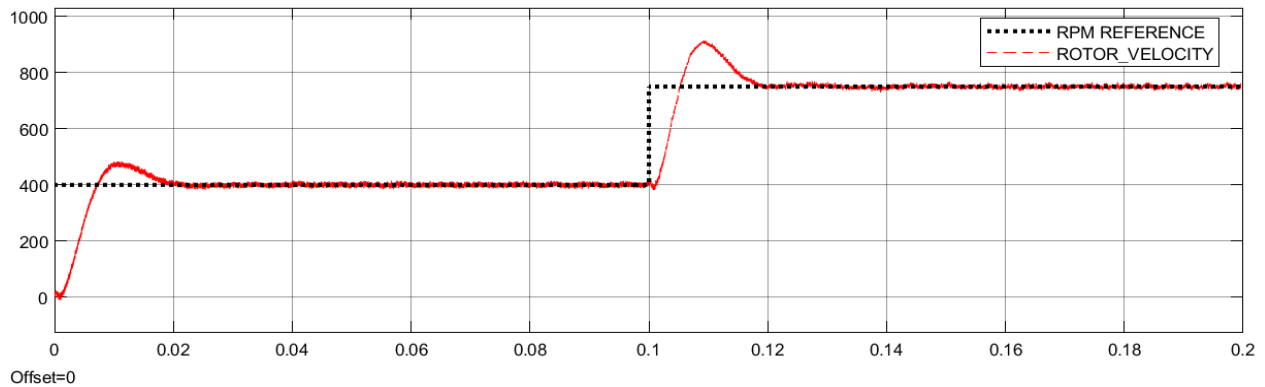
MODEL REFERENCE ADAPTIVE SYSTEM (MRAS) is used to develop the sensorless vector control of PMSM is tested under different test conditions. SMC controller is used as adaptive control law.

In this section speed control of PMSM is implemented in sensorless mode. Two test cases are tested on simulated in this project.

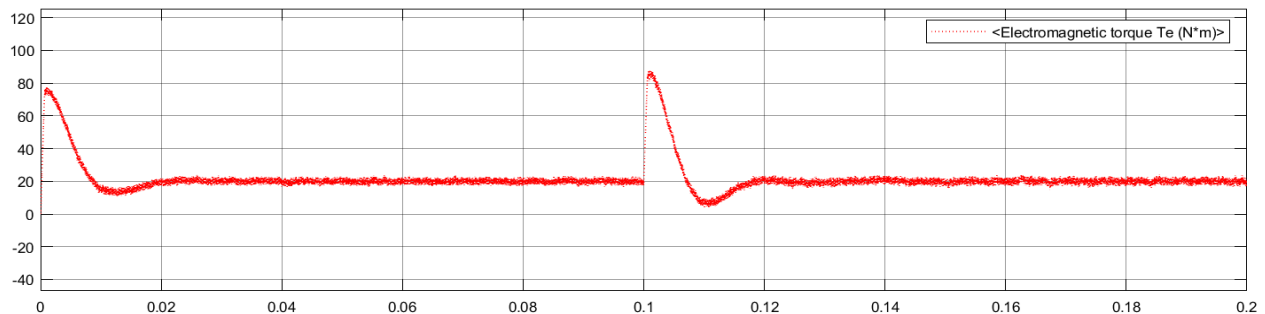
1. The speed reference is changed from 0 to 400 rpm at 0 s and from 400 rpm to 750 rpm with rated load torque of 20 Nm.
2. The torque load is changed from 20 Nm to 10 Nm with rated speed of 750 rpm.

These test cases are satisfactorily test the performance of motor under the various loading conditions. Simulation should mirror the performance of the drive in real world conditions.

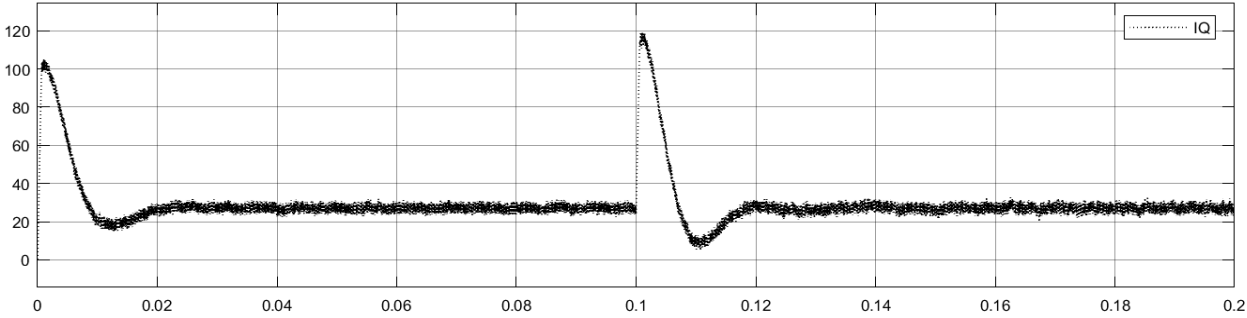
- 1. The speed reference is changed from 0 to 400 rpm at 0 s and from 400 rpm to 750 rpm with rated load torque of 20 Nm**



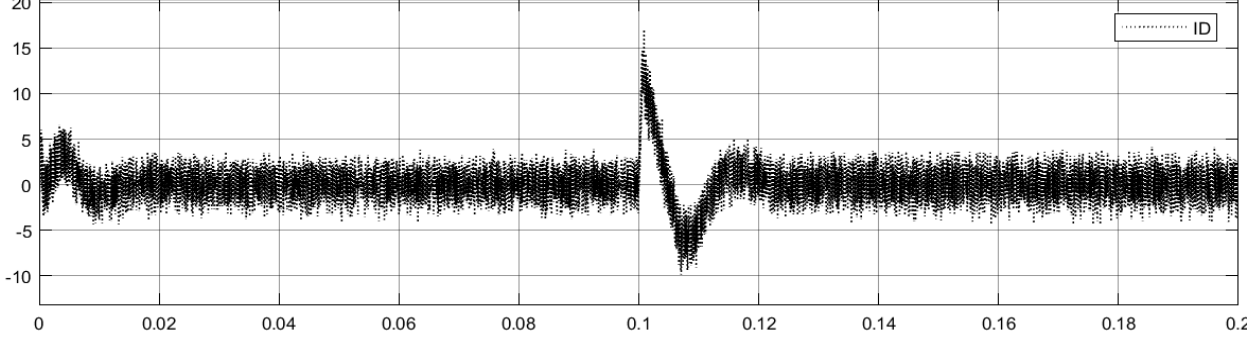
### 6.2 Rotor Velocity



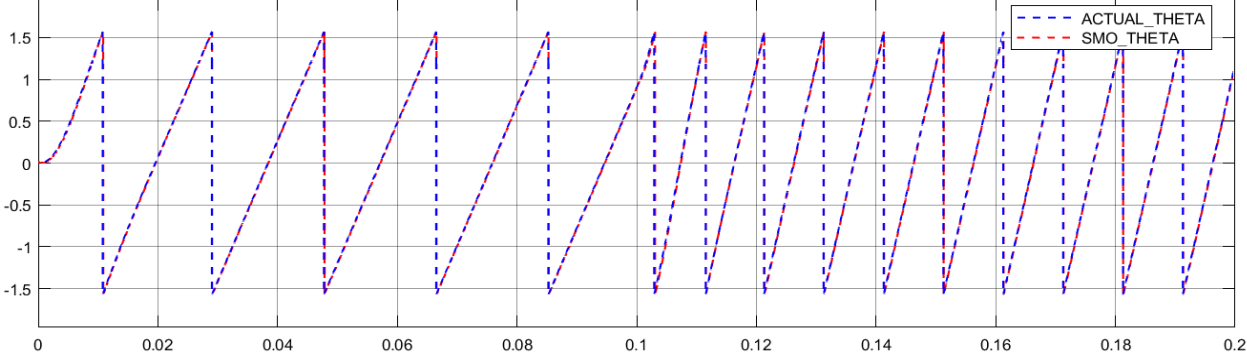
### 6.3 Electromagnetic Torque



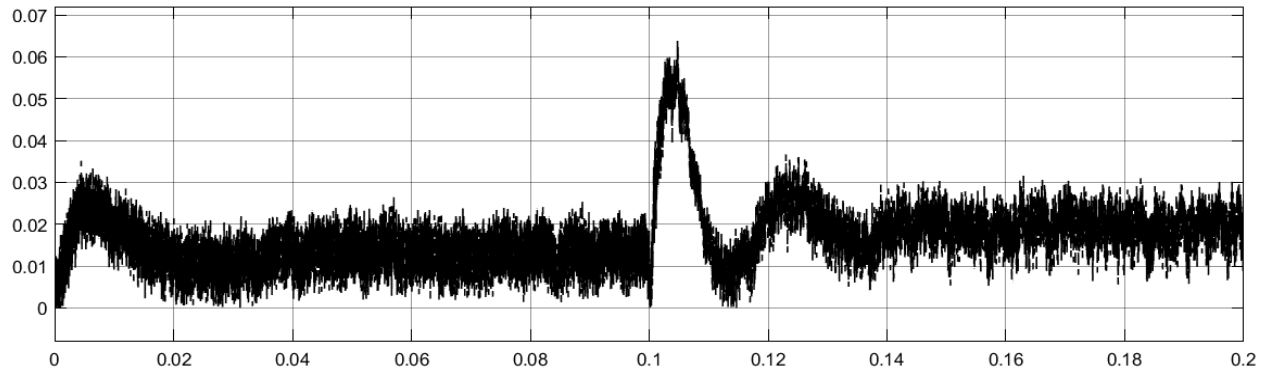
### 6.4 Iq Current



### 6.5 Id Current



### 6.6 Rotor Angle



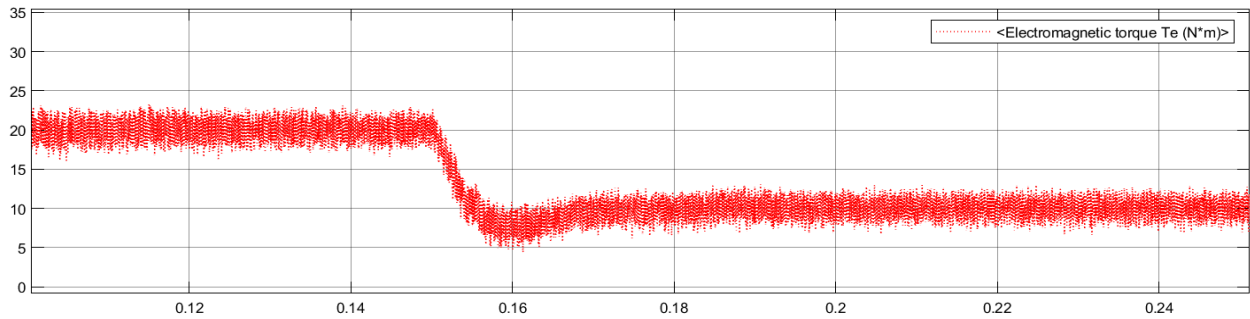
## 6.7 Rotor Angle Error

Figure 6.2 shows the rotor velocity response when the speed reference is changed from 0 to 400 rpm at 0 s and from 400 rpm to 750 rpm at 0.1s with rated load torque of 20 Nm. The rotor velocity response is as good as response obtained in SMO as in Figure 5.4. Figure 6.3 , figure 6.4 and figure 6.5 shows the electromagnetic torque , Iq and Id current. Figure 6.6 and 6.7 shows the comparison of estimated rotor angle and actual rotor angle and rotor angle error.

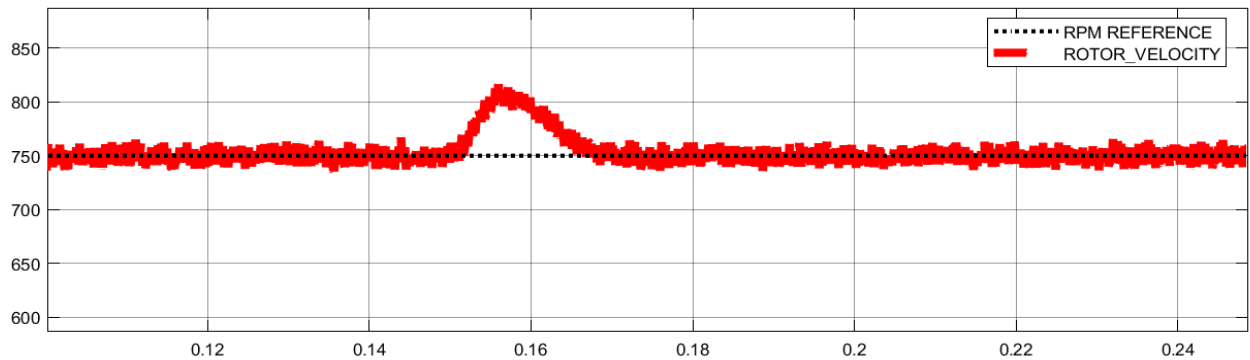
As shown in figure 6.7, the maximum rotor angle error deviation is significantly less than SMO (figure 5.11 and figure 5.29). From the above ,it can be inferred that dynamic performance of model reference adaptive system is better than SMO.



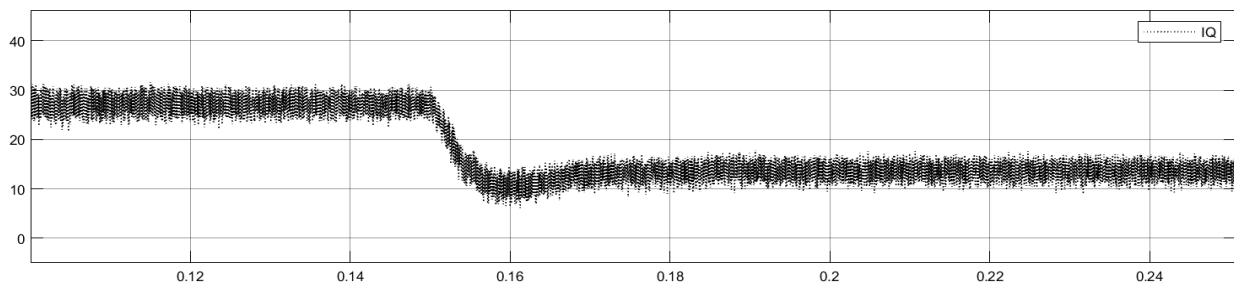
1. The torque load is changed from 20 Nm to 10 Nm with rated speed of 750 rpm



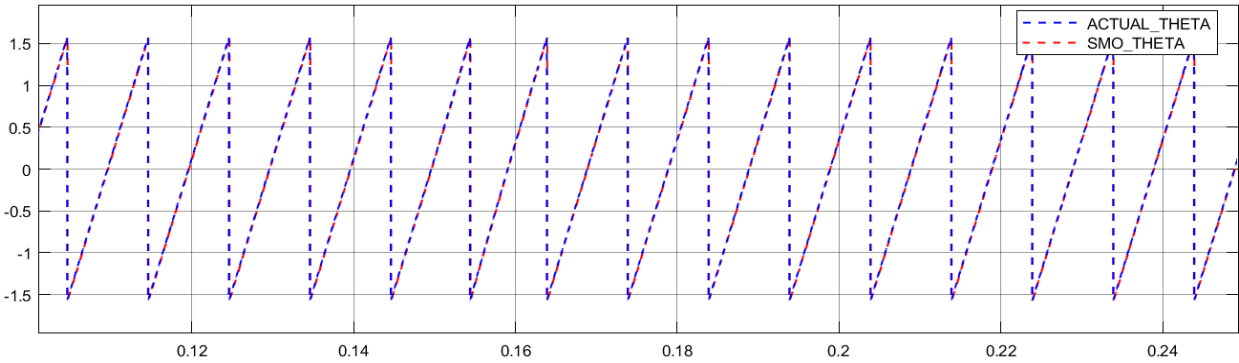
6.8 Electromagnetic Torque



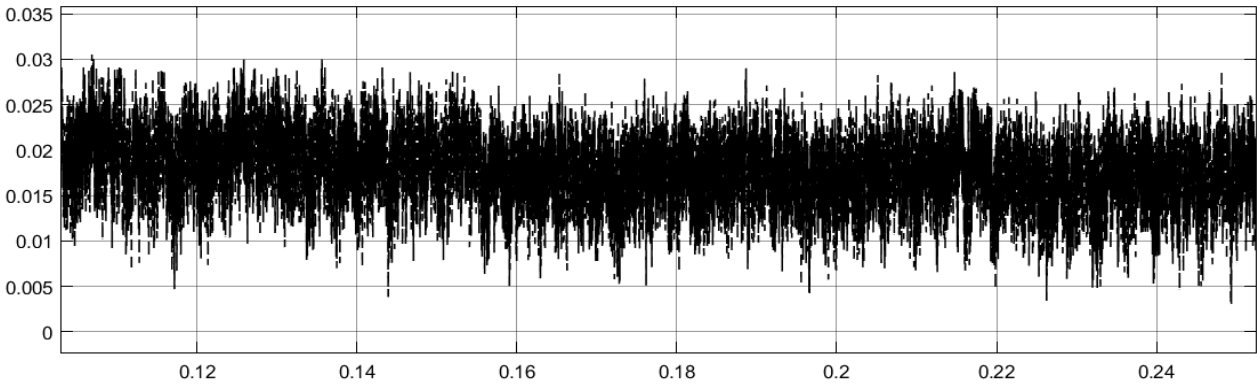
6.9 Rotor Velocity



### 6.10 Iq Current



### 6.11 Rotor Angle



### 6.12 Estimated Rotor Angle Error

The rotor angle between the actual rotor angle and estimated SMO rotor angle is compared and error b/w them is displayed figure 6.11 and 6.12, it is observed that there is no significant deviation in estimated rotor angle from true rotor angle deviation when the motor is in transient state. It is shown that the estimated rotor angle is as good as the new SMO developed in the project

## 6.4. Discussion

SMO are known for their robust nature against the parameter variation and disturbance due to which they are preferred choice in sensorless control. Conventionally SMO is used with signum function but chattering is a major problem in sliding mode . In this project modified SMO is used with saturation function to mitigate the effect of chattering. But the presence of lpf deteriorates the dynamic performance of SMO as it introduces the time delay in the system. Hence, a modified SMO is designed with back emf observer. The dynamic performance of the two observer is tested under two test conditions in section 5.2.5 and 5.3.5.

The modified SMO shows promising result as the deviation of estimated rotor angle from the actual rotor angle in transient state is also reduced as in figure 5.11 and 5.29. Steady state performance of new improved SMO is shown at 400 rpm and 750 rpm as in figure 5.15, 5.18 ,5.16, 5.19, 5.35 5.38, 5.36 and 5.39 respectively which shows excellent stator current tracking ability of sliding mode controller. But the estimated rotor angular velocity has oscillation in transient state as in figure 5.26

The rotor angle estimation depends upon the back emf of motor but at low speed the resolution of back emf is low as it directly proportional to the speed. Hence, the low speed operation is a major problem and a starting method is also required. Therefore, for this reason provided motivation for work on another sensorless control based on MRAS which provided wide speed operation of sensorless control. A MRAS based sensorless control is simulated. The sliding mode controller is used as adaptive law to improve the performance. The dynamic performance of MRAS is tested under two different testing conditions as mentioned in section 6.4 .

As in figure 6.2, the estimated rotor angular velocity is improved significantly in comparison to figure 5.26 of the modified SMO. Maximum estimated rotor angle error deviation in dynamic condition is between the error of both the SMO as in figure 6.7 , 5.11 and 5.29.

Although, the wide speed operation is possible but the dependence of MRAS on motor state variable model is a major problem. In [5], this problem is solved by estimating the motor parameter during the operation.

## CHAPTER 7

### 7.1 CONCLUSION

The main of this project is to implement different sensorless techniques for sensorless vector control of PMSM. A new modified SMO based sensorless control is presented, which improves the performance of motor. MRAS based sensorless technique is developed.

In the second chapter, various several sensorless techniques available in the literature are discussed and compared. With the present available resources and estimator performance, two estimator are best suited: SMO and MRAS are simulated. SMO is developed and simulated. Further, a modified SMO is developed to further improve the performance.

FOC requires the rotor angle and speed which is fed through the sensors such as encoder and resolver. In sensorless control, the rotor angle and speed are estimated by estimators. These estimation techniques are the focus of this thesis. Several estimator are studied and compared on various parameters. FOC with various estimators are modelled in the SIMULINK.

In the third chapter mathematical modelling of PMSM is done in abc, dq and  $\alpha\beta$  coordinates with park and clark transformation. SVPWM switching control technique is explained.

In the fourth chapter, FOC of PMSM is implemented in Matlab. Speed control is implemented with three PI. The performance of the motor is tested under various dynamic condition.

In the fifth chapter, Two different SMO are discussed. With one observer further enhancing the performance of the of former. SMO's mathematical modelling is discussed with their stability condition. FOC with SMO are modelled in Simulink.

In the sixth chapter, MRAS for sensorless control is discussed. MRAS's mathematical modelling is discussed with its stability condition. Sensorless FOC with MRAS is modelled in Simulink and tested under various test condition

Based on the results from the modelling and simulations, the MRAS estimation method provide wide speed operation and less rotor angle deviation best suited for the case study.

## 7.2. FUTURE WORK

The MRAS is more preferred than SMO due to its wide speed operation and less estimated rotor angle deviation in transient state .But, MRAS depend on the rotor parameter for speed estimation, which varies during the operation. Therefore, a system must be developed to estimate the rotor parameter in MRAS.

SMO requires an algorithm at the starting which can be further investigated in order to improve the starting performance of the motor. Analyses is required for the measurement accuracy at the low speed. SMO can be complemented to closed loop speed estimator such as PLL and MRAS to further enhance the performance

Implementation of the controller on a hardware is preferred. Analysis of test conditions on the real motor would be preferred in comparison to sensors i.e. encoder.

## References

1. S. Chi, Z. Zhang and L. Xu, "Sliding-Mode Sensorless Control of Direct-Drive PM Synchronous Motors for Washing Machine Applications," in *IEEE Transactions on Industry Applications*, vol. 45, no. 2, pp. 582-590, March-april 2009, doi: 10.1109/TIA.2009.2013545.
2. H. Kim, J. Son and J. Lee, "A High-Speed Sliding-Mode Observer for the Sensorless Speed Control of a PMSM," in *IEEE Transactions on Industrial Electronics*, vol. 58, no. 9, pp. 4069-4077, Sept. 2011, doi: 10.1109/TIE.2010.2098357.
3. Z. Qiao, T. Shi, Y. Wang, Y. Yan, C. Xia and X. He, "New Sliding-Mode Observer for Position Sensorless Control of Permanent-Magnet Synchronous Motor," in *IEEE Transactions on Industrial Electronics*, vol. 60, no. 2, pp. 710-719, Feb. 2013, doi: 10.1109/TIE.2012.2206359.
4. C. Gong, Y. Hu, J. Gao, Y. Wang and L. Yan, "An Improved Delay-Suppressed Sliding-Mode Observer for Sensorless Vector-Controlled PMSM," in *IEEE Transactions on Industrial Electronics*, vol. 67, no. 7, pp. 5913-5923, July 2020, doi: 10.1109/TIE.2019.2952824
5. O. C. Kivanc and S. B. Ozturk, "Sensorless PMSM Drive Based on Stator Feedforward Voltage Estimation Improved With MRAS Multiparameter Estimation," in *IEEE/ASME Transactions on Mechatronics*, vol. 23, no. 3, pp. 1326-1337, June 2018, doi: 10.1109/TMECH.2018.2817246
6. A. Mishra, V. Mahajan, P. Agarwal and S. P. Srivastava, "MRAS based estimation of speed in sensorless PMSM drive," 2012 IEEE Fifth Power India Conference, Murthal, 2012, pp. 1-5, doi: 10.1109/PowerI.2012.6479492
7. Wang Zhifu, Teng Qizhi and Zhang Chengning, "Speed identification about PMSM with MRAS," 2009 IEEE 6th International Power Electronics and Motion Control Conference, Wuhan, 2009, pp. 1880-1884, doi: 10.1109/IPEMC.2009.5157702
8. Y. Shi, K. Sun, L. Huang, and Y. Li, "Online identification of permanent magnet flux based on extended Kalman filter for IPMSM drive with position sensorless control," *IEEE Trans. Ind. Electron.*, vol. 59, no. 11, pp. 4169-4178, Nov. 2012.
9. G. R. GoPinath and P. D. Shyama, "Sensorless control of PMSM using an adaptively tuned SCKF," in *The Journal of Engineering*, vol. 2019, no. 17, pp. 4304-4308, 6 2019, doi: 10.1049/joe.2018.8081.
10. Z. Wang, Y. Zheng, Z. Zou and M. Cheng, "Position Sensorless Control of Interleaved CSI Fed PMSM Drive With Extended Kalman Filter," in *IEEE Transactions on Magnetics*, vol. 48, no. 11, pp. 3688-3691, Nov. 2012, doi: 10.1109/TMAG.2012.2197180.
11. S. Bolognani, L. Tubiana and M. Zigliotto, "Extended Kalman filter tuning in sensorless PMSM drives," in *IEEE Transactions on Industry Applications*, vol. 39, no. 6, pp. 1741-1747, Nov.-Dec. 2003, doi: 10.1109/TIA.2003.818991
12. <https://auto.economicstimes.indiatimes.com/news/auto-components/high-efficiency-gains-to-spur-use-of-pm-motor-in-future-ev-designs-report/72317517>

13. L. Jiayi, Y. Guijie and Y. Pengfei, "Rotor Position Estimation for PMSM Based on Sliding Mode Observer," 2007 International Conference on Mechatronics and Automation, Harbin, 2007, pp. 3684-3689, doi: 10.1109/ICMA.2007.4304159.
14. Kye-Lyong Kang, Jang-Mok Kim, Keun-Bae Hwang and Kyung-Hoon Kim, "Sensorless control of PMSM in high speed range with iterative sliding mode observer," Nineteenth Annual IEEE Applied Power Electronics Conference and Exposition, 2004. APEC '04., Anaheim, CA, USA, 2004, pp. 1111-1116 vol.2, doi: 10.1109/APEC.2004.1295961
15. .V. Utkin, J. Guldner, and J. Shi, *Sliding Mode Control in Electromechanical Systems*, 1st ed. New York: Taylor & Francis, 1999, ch. 8.
16. B. K. Bose and B. Bose, "Power electronics and motion control—Technology status and recent trends," IEEE Trans. Ind. Appl., vol. 29,no. 5, pp. 902–909, Sep./Oct. 1993.
17. Vas, P. (1998). *Sensorless vector and direct torque control*. Oxford: Oxford University Press.
18. Dianguo Xu, Gaolin Wang, and Guo-Qiang Zhang,"Position Sensorless Control Techniques for Permanent Magnet Synchronous Machine Drives"